THE PENNSYLVANIA STATE UNIVERSITY
SCHREYER HONORS COLLEGE

DEPARTMENT OF BIOCHEMISTRY AND MOLECULAR BIOLOGY

Use of Recombinant Urocanase to Study the Inhibitory Effects of Imidazolone Propionate Breakdown Products on Aspartate Aminotransferase

ISABELLA RUUD
SPRING 2022

A thesis
submitted in partial fulfillment
of the requirements
for a baccalaureate degree
in Biochemistry and Molecular Biology
with honors in Biochemistry and Molecular Biology

Reviewed and approved* by the following:

Allen Phillips
Professor Emeritus of Biochemistry
Thesis Supervisor

Lorraine Santy
Associate Professor of Biochemistry and Molecular Biology
Honors Adviser

* Electronic approvals are on file.

ABSTRACT

A deficiency in imidazolonepropionase (IPase), an enzyme in the pathway catabolizing histidine to glutamate, has been previously shown to cause an oxygen-dependent growth reduction in *Escherichia coli* cells (Kabeer, 2000). The growth reduction is thought to be caused by an inhibition of aspartate aminotransferase (AAT) as a result of oxidative breakdown of the accumulated substrate for IPase, imidazolone propionate (IoPA). In order to investigate this potential causation of growth reduction, a recombinant 6-His-tagged version of urocanase, the enzyme that synthesizes IoPA, was established. Optimization of the expression and subsequent purification of this urocanase provided sufficient yields of pure enzyme to study the specificity of urocanase for its tightly bound nicotinamide adenine dinucleotide (NAD^+) cofactor. In addition, the His-tagged urocanase allowed enzymatic synthesis of IoPA and one of its breakdown products, α-ketoglutaramate (α-KGM), through immobilization of the enzyme on Ni^{+2}-binding beads. Following purification of each synthesis product, assays of AAT activity from *E. coli* crude extract in the presence of these compounds showed a decrease in AAT specific activity corresponding to increased amounts of α-KGM. Through the use of recombinant urocanase enzyme, the effect of IoPA and α-KGM on AAT have been characterized that point to a model of inhibition that ultimately causes a reduction in *E. coli* growth.

TABLE OF CONTENTS

LIST OF FIGURES

LIST OF TABLES

ACKNOWLEDGEMENTS

I would first like to thank Dr. Allen Phillips for his support, guidance, and wisdom throughout all stages of conducting the research for and writing this thesis. I have learned a tremendous amount through his training on how to design experiments, analyze data, and communicate results. I will always be grateful to have received my fundamental scientific training from Dr. Phillips. I would also like to thank the Biochemistry and Molecular Biology Department and the PA NASA Space Grant Consortium for assistance in funding this research. Finally, I am grateful to my family and friends who have supported me throughout this entire process.

Chapter 1

Introduction

The catabolism of L-histidine is a well-studied metabolic process in organisms ranging from bacteria to plants to humans. Histidine's utilization (Hut) pathway, leading to L-glutamate as the principal carbon product, initially involves the action of three enzymes: histidase (histidine ammonia-lyase, EC 4.3.1.3) performs a non-oxidative deamination of histidine to *trans*-urocanate plus ammonia, and is followed by urocanase (urocanate hydratase, EC 4.2.1.49) that acts on *trans*-urocanate through a unique NAD^+-dependent addition of water to result in formation of imidazolone propionate (IoPA); the lesser studied imidazolonepropionase (IPase), EC 3.5.2.7, then hydrolytically opens the IoPA ring to produce formiminoglutamate (FIGLU). Subsequent reactions by which FIGLU proceeds to glutamate differ among the organisms involved, but in all cases the process results in formation of glutamate, a 1-carbon product, and ammonia nitrogen. The work described here primarily concerns the urocanase and IPase enzymes because their functionality in this pathway is linked and much remains to be learned about the details of their catalysis in histidine catabolism.

Interestingly, both histidase and urocanase are enzymes that possess unusual coenzymes to carry out their catalytic function. In the case of histidase, its active center is generated during the folding of each of four identical protein subunits by a spontaneous cyclization of a short sequence of 3 amino acids (Ala-Ser-Gly) present in the protein backbone's sequence (Hernandez & Phillips, 1994). Although not fully understood in detail, this results in the formation of 4-methylidene-imidazole-5-one (MIO), a novel electrophilic co-factor that is found in all histidases

examined thus far but which remains to be identified in other ammonia-lyase enzymes except for some phenylalanine ammonia-lyases (Langer et al., 2001). On the other hand, work originating in this laboratory discovered that urocanase contains a well-known coenzyme, NAD^+, tightly but non-covalently bound to the enzyme's protein (Egan & Phillips, 1977). Moreover, NAD^+ function in this reaction has been shown to be different from that observed in all other NAD^+-dependent reactions. And because all urocanase enzymes studied in detail have contained tightly bound NAD^+, this coenzyme requirement appears unchanged through evolutionary times. The work covered here explores the specificity for NAD^+ binding in urocanase from *Pseudomonas putida,* although that enzyme is now recombinantly produced in *Escherichia coli* that lack the Hut pathway but contain a plasmid holding a cloned version of the *hutU* gene from *P. putida*.

There have been numerous genetic studies involving humans lacking histidase, a relatively common condition termed histidinemia, and also some but fewer involving urocanase; both conditions may result in mental deficiency, but these are only rarely life-threatening and a majority of persons so afflicted experience normal life spans (La Du, 1967 and Kalafatic et al., 1980). On the other hand, there have been no known reports of persons lacking IPase activity (Lam et al., 1996, Espinós et al., 2009). On the surface, this observation can be rationalized by recognition that humans can make FIGLU from alternative routes involving methenyl-tetrahydrofolate and glutamate, but does not explain the total absence of persons excreting IoPA as a result of having no IPase activity. Thus, the question of the essential need for IPase in humans remains unanswered, but perhaps the importance of IPase can be understood from an examination of simpler microbial systems.

Previous work performed in this laboratory (Kabeer, 2000) showed that when *E. coli* cells containing histidase and urocanase activity but lacking IPase activity (necessary to convert

IoPA to FIGLU) were grown under anaerobic conditions with histidine present, the cells exhibited growth at the expected rate, but if anaerobic growth was interrupted by oxygen introduction into the growth environment, under those oxygenated conditions the cells ceased to grow, suggesting that accumulated IoPA itself is a growth-inhibitory compound when oxygen is present, or else IoPA is converted by oxygen to a compound that is itself inhibitory. Considerable chemistry has been done on IoPA and its instability in the presence of oxygen at neutral pH is documented. While several products can be formed under such conditions, none have been studied for a possible inhibitory effect on growth of *E. coli* cells. Work described here examines IoPA and a compound, α-ketoglutaramate, formed from IoPA in the presence of oxygen, to determine if either of these would inhibit aspartate aminotransferase and thus by the loss of that important Citric Acid Cycle enzyme's activity, explain the cell growth decline as a direct result.

Chapter 2

Literature Review

2.1 Histidine Degradation Pathway

The ability to break down histidine into glutamate, ammonia, and a one-carbon compound (either formate or formamide) is almost universal among organisms. The first three steps are highly conserved: histidase eliminates an ammonia from histidine to yield urocanate, water is added across a double bond in urocanate to result in imidazolone propionate (IoPA) upon urocanase action, and IPase cleaves the ring in imidazolone propionate to synthesize formiminoglutamate (FIGLU) (Bender, 2012). After the creation of formiminoglutamate, the final steps of the pathway depend on the organism, but they generally follow a common scheme depending on whether the organism subscribes to the four or five-step pathway.

In the four-step pathway, used by microorganisms like *Klebsiella aerogenes*, a single enzyme, FIGLU formiminohydrolase, hydrolyzes FIGLU to yield glutamate and formamide (Magasanik & Bowser, 1955). In eukaryotic organisms, the four-step pathway is coupled with folate metabolism such that the formimino group of FIGLU is transferred to the N5 position of 5,6,7,8-tetrahydrofolate by formiminotranferase cyclodeaminase (FTCD), resulting in glutamate and 5-formimidoyltetrahydrofolate (Mao et al., 2004). FTCD is a bifunctional enzyme that channels 5-formimidoyltetrahydrofolate into a cyclization reaction that generates ammonia and N5, N10-methenyl-THF, an important precursor for other folate coenzymes (Mao et al., 2004).

The five-step pathway differs from the four-step pathway by the generation of an additional mole of ammonia; thus, the nitrogen in histidine is better utilized in this pathway. However, fewer microorganisms use this pathway, such as *Pseudomonas fluorescens* (Tabor &

Mehler, 1954). Here, the imino group of FIGLU is hydrolyzed by FIGLU iminohydrolase yielding ammonia and formylglutamate (FG). FG is then acted on by FG amidohydrolase to complete the pathway with the formation of formate and glutamate (Tabor & Mehler, 1954).

Human disorders arising from a deficiency in three of the enzymes involved in the four-step pathway have been identified. Histidinemia is a result of lacking a functional histidase, the first enzyme in the pathway. The disorder is characterized by high blood histidine levels, low amounts of urocanate in the sweat, and varying degrees of speech and mental impairment (La Du, 1967). In a similar manner, a urocanase deficiency has been shown to lead to mental deficits and ataxia in some, but not all, cases (Kalafatic et al., 1980). Defects in the FTCD enzyme have been linked to disorders displaying a high level of FIGLU in the urine that can have severe phenotypes like megaloblastic anemia, delayed development, and cognitive impairment (Hilton et al., 2003). Interestingly, there are no recorded cases of patients lacking IPase activity. Low expression of *AMDHD1*, the human gene for IPase, was identified in a comparative microarray analysis looking at Hemochromatosis Type 2b (Song et al., 2013). This disorder is characterized by a buildup of iron that causes heart, liver, and pancreas damage, but no further studies on its relation to IPase have been conducted. It thus remains of interest whether such deficiencies of IPase exist, or if such a deficiency results in a phenotype incompatible with life.

To study the genes associated with these enzymes, histidine utilization genes from *Pseudomonas putida*, which employs the five-step pathway, have been cloned into *E. coli* by this lab (Consevage & Phillips, 1990). Sarfaraz Kabeer used one of these original constructs to move the *hutH* and *hutU* genes encoding histidine and urocanase, respectively, to a BlueScript vector that constitutively expressed the genes under the chosen conditions (Kabeer, 2000). One strain contained just the *hutH* gene and another contained both *hutU* and *hutH*. Work by Kelly Helfrich

in 2011 took the *hutU* gene and cloned it into a pET17b vector for overexpression. Further developments made by Steven Davis in 2016 used Helfrich's construct to move the *hutU* gene to a pET28b vector. This change allowed for *hutU* expression under control of the *lac* operon's repressor and the addition of a N-terminal 6-His tag, facilitating simple purification of urocanase.

2.2 Urocanase

Urocanase, also referred to as urocanate hydratase or imidazolone-propionate hydrolase, is the second enzyme in the pathway catabolizing histidine to glutamate (Tabor et al.,1952). After histidine loses ammonia to form urocanate, urocanate is then hydrated by urocanase to yield hydroxy-imidazole-propionate which is converted to imidazolone propionate through spontaneous tautomerization (Kessler et al., 2004). Urocanase utilizes NAD^+ as a coenzyme, to which it binds tightly enough to necessitate denaturing conditions to remove enzyme-bound NAD^+ (Egan & Phillips, 1977). Because of this strong association, NAD^+ must be present upon protein folding to be incorporated into the enzyme, and it cannot be added after the fact.

The structure of the enzyme consists of two identical subunits, each composed of 557 amino acids for a molecular weight of 60,781 Da. Solved crystal structures revealed that each subunit contains an NAD^+ binding domain located in a larger domain that sequesters urocanate, NAD^+, and five water molecules, one of which is necessary for substrate hydration during catalysis (Kessler et al., 2004). The bound NAD^+ is able to form adducts that reduce the activity of the enzyme, where a urocanase with two NAD^+-nucleophile adducts has less activity compared to the version with one NAD^+ adduct and one intact NAD^+ or two intact NAD^+

molecules, which has the highest specific activity (Klepp & Retey, 1989). Using HPLC, the three forms can be separated, and by irradiation at 320 nm, the less active forms can be photoactivated to a more active version by removing the adduct on bound NAD^+ molecules (Klepp & Retey, 1989).

While most enzymes that utilize NAD^+ are dehydrogenases that catalytically rely on the power of NAD^+ as an oxidizing agent, urocanase uses the cofactor in a unique way. It was originally thought that the mechanism relied on an internal oxidation-reduction process, but further investigation revealed a more likely mechanism by which NAD^+ forms a covalent addition complex with a nitrogen in the imidazole ring of urocanate (Egan et al., 1981). The delocalization of electrons in the imidazole ring then supports the addition of a water molecule across the double bond to form imidazolone propionate (Egan et al., 1981).

Other enzymes using NAD^+ as a cofactor have been extensively studied to determine if analogs of NAD^+ are sufficient for catalysis, but no such studies have been conducted on urocanase. Glyceraldehyde 3-phosphate dehydrogenase, the enzyme responsible for catalyzing the sixth step of glycolysis where glyceraldehyde 3-phosphate is oxidized to 1,3-bisphosphoglycerate, is able to use thionicotinamide adenine dinucleotide (thio-NAD^+), acetylpyridine adenine dinucleotide, and nicotinamide hypoxanthine dinucleotide (NHD^+) for sufficient catalytic purposes (Eby & Kirtley, 1971). Both thio-NAD^+ and acetylpyridine adenine dinucleotide contain chemical modifications in the nicotinamide moiety. In comparison, NHD^+ contains an altered adenosine moiety. All three of these analogs also could be used as substrates like NAD^+ in both glutamate dehydrogenase and alcohol dehydrogenase, as well (Biellmann et al., 1974).

2.3 Imidazolone Propionate

Imidazolone propionate (IoPA) is produced by the enzymatic activity of urocanase on urocanate. Evidence of its structure was originally very difficult to obtain because of the instability of 4-imidazolones, which can only be stabilized in anaerobic, dark, acidic conditions. Eventual characterization of IoPA revealed it has a half-life of 24 minutes in aerobic neutral conditions but is stable for days in acidic environments (Brown & Kies, 1959b).

In oxygen there are several potential breakdown products of IP. One possible outcome is non-oxygen-dependent hydrolysis to produce N-formylisoglutamine, which can be further hydrolyzed to isoglutamine. Despite the lack of reliance on oxygen for this mechanism, it has been reported that it does not occur in anaerobic environments (Rao & Greenberg, 1961). Alternatively, oxidation of IoPA followed by hydrolysis yields 4-ketoglutaramate, ammonia, and formate as final products (Matherly & Phillips, 1980). Additionally, in higher organisms, hydantoin-5-propionate can also be formed from IoPA through an oxygen-dependent enzymatic mechanism (Brown & Kies, 1959a).

Studies looking at the histidine-utilization in *Salmonella typhimurium* showed that in strains lacking *hutI*, the gene encoding IPase that breaks down IoPA, there was an observed growth inhibition (Bochner & Savageau, 1979). Further growth studies on tetrazolium indicator plates pointed towards inhibition of aspartate aminotransferase as a potential cause for the growth reduction. These results were further supported by *E. coli* aspartate aminotransferase mutants displaying similar poor growth patterns on succinate minimal media that could be rescued by the same amino acids that relieve IoPA-mediated growth inhibition (Bochner & Savageau, 1979).

Building on these results, studies were done in *E. coli* to determine if IoPA-mediated growth inhibition could be transferred to an organism that does not naturally contain this histidine utilization pathway. The strain that contained the *hutH* and *hutU* genes showed a reduction in growth rate on succinate + histidine minimal media, but not the strain containing only the *hutH* gene (Kabeer, 2000). Only the strain containing both *hutH* and *hutU* can form IoPA from histidine, but not the strain with only *hutH*, thus indicating a build-up of IoPA as a cause for growth reduction. Interestingly, this reduction in growth was only seen when the strains were grown in the presence of oxygen; if grown anaerobically, no growth issues were observed (Kabeer, 2000). The added evidence of oxygen dependence points towards an oxidative breakdown product of IoPA acting as the inhibitory compound potentially targeting aspartate aminotransferase.

2.4 Aspartate Aminotransferase

Aspartate aminotransferase is a metabolic enzyme that catalyzes the transfer of an amino group from aspartate to α-ketoglutarate to form glutamate and oxaloacetate. The reverse reaction is also possible, where an amino group from glutamate is transferred to oxaloacetate to form aspartate and α-ketoglutarate (Kirsch et al., 1984). The enzyme consists of two identical subunits that each contain a large domain to bind the pyridoxal phosphate coenzyme, a small domain to shift the conformation of the enzyme from open to closed forms, and an N terminal domain to stabilize the dimer (Kirsch et al., 1984). The interface of the two subunits forms the active site where upon substrate binding, the enzyme shifts into the closed conformation to tighten the active site pocket for the transamination reaction (Kirsch et al., 1984).

Aspartate aminotransferase is heavily tied to energy metabolism through its role in the malate-aspartate shuttle. The malate-aspartate shuttle acts to transfer reducing equivalents generated from glycolysis in the cytosol to the matrix of the mitochondria. NADH formed in the cytosol is used to reduce oxaloacetate to form NAD^+ and malate, where the latter then is transported into the mitochondria. Malate dehydrogenase oxidizes malate to generate NADH and oxaloacetate in the mitochondria, thus completing the transfer of reducing power (Safer, 1975). For this cycle, to continue, oxaloacetate must be returned to the cytosol, but without a membrane transporter to allow it to cross the outer mitochondrial membrane, it must first be transaminated by aspartate aminotransferase to generate aspartate. The aspartate can cross the membrane through a carrier system where it can be transaminated in the reverse reaction by aspartate aminotransferase to return oxaloacetate to the cytosol (Safer, 1975). Without a properly functioning malate-aspartate shuttle, oxidative phosphorylation is affected and ATP production drops (Kaupinnen et al., 1987).

Because prokaryotes do not rely on this shuttle, the primary role of aspartate aminotransferase is in the formation of amino acids like aspartate. Aspartate can then be used to make many other amino acids like methionine, threonine, isoleucine, and asparagine (Miesack & Coruzzi, 2002). Beyond amino acids, aspartate is a precursor for the biosynthesis of other important metabolites like NAD^+, vitamin B5, and nucleotides (Liu et al., 2014). *E. coli* display a close relationship between amino acid and sugar metabolism, suggesting that aspartate aminotransferase also has an influence on energy production. Both oxaloacetate and α-ketoglutarate, compounds that are acted on by aspartate aminotransferase, have been shown to impact glucose uptake and catabolism (Zampieri et al., 2019). Finally, both of these compounds

are intermediates in the citric acid cycle, which is important for generating energy and reducing power (Kornberg, 1966).

In addition, it has been shown in *E. coli* that the absence of aspartate aminotransferase leads to slower cell growth and smaller cells (Liu et al., 2014). Only the addition of aspartate, out of all of the amino acids, could reverse this effect. The likely mechanism behind this growth was by means of changes in cell cycle regulation through modulating the levels of initiator protein DnaA. In order to replicate the chromosome, a complex of 20 DnaA molecules bind to the origin of replication in the early stages of DNA replication and induces unwinding that allows for other replication machinery to bind (Margulies & Kaguni, 1996). The decreased levels of aspartate aminotransferase led to diminished levels of DnaA protein per cell, thus reducing the ability of the cell to replicate DNA and divide (Liu et al., 2014).

Chapter 3

Materials and Methods

3.0 Construction of pSD22

Two former undergraduate students in this laboratory, Kelly Helfrich and Steven Davis, were actively involved in work leading to the plasmid pSD22 that was used for research described in this thesis. Their work has not been published but the methods used are described here in sufficient detail to summarize how the desired pSD22 plasmid construct originated. Helfrich cloned the *hutU* gene into a commercial vector from Novagen, pET17, maintained in *E. coli* DH5α; the source of that gene was from one of several constructs available in this laboratory that contained the *hutU* gene, all such constructs having been derived previously from the cloning into *E. coli* of the entire collection of *hut* genes present in *Pseudomonas putida* ATCC 12633 (Consevage & Phillips, 1990).

In construction of a plasmid designed to overproduce the native urocanase protein, Helfrich employed a site-directed mutagenesis (SDM) kit to create a new NdeI site, CATATG, at the urocanase start codon by replacing the first G base contained in the urocanase start codon (GTG) with an A base, thereby producing a NdeI site with an improved (ATG) start codon for urocanase gene translation. The intent was to clone the *hutU* gene between an existing NdeI site present in pET17 and a BamHI site found in the multi-site cloning region of pET17. Helfrich then used SDM to create a BamHI site roughly 13 bases following the TGA stop codon used to end translation of the *hutU* gene. When the final NdeI – BamHI fragment containing the *hutU* gene was ligated into a similarly cut pET17, and the resulting plasmid transformed into an

appropriate *E. coli* DH5α host strain, urocanase activity was observed. That plasmid is referred to here as pKH7.

Following the Helfrich work, Steven Davis took the next steps to clone a tagged version of the *hutU* gene for high level expression of urocanase that could be purified in a one-step procedure using an immobilized metal-attached column (IMAC) procedure. Davis employed a different plasmid vector, pET28a, in order to achieve this result. Use of the pET28a vector simply involved removing the NdeI – BamHI fragment from the Helfrich pKH7 urocanase-gene construct by digestion with those two restriction endonucleases, gel-purifying the desired gene fragment, and then moving that into pET28a that had been cleaved by these two restriction enzymes to allow ligation of the urocanase-containing fragment between those two sites, thus resulting in the pSD22 plasmid.

The resulting transcript of the *hutU* gene was designed to start at the ATG codon contained in the NcoI site (CCATGG) and followed by the 6 histidine codons, thereafter encountering, in the appropriate reading frame, the entire *hutU* gene coding region located between the nearby NdeI site and the distant BamHI site that followed the *hutU* stop codon. These features designed into pSD22 were ones needed to allow high level expression of the urocanase gene and to produce a protein with a 6-His-tagged region that was suitable for single step purification of urocanase using an IMAC column. DNA sequence results confirming the plasmid's DNA features were performed by the Nucleic Acid Facility at Penn State for this thesis and are also presented in the Results section.

3.1 Bacterial Crude Extract Preparation

3.1.1 Culture Growth

For the urocanase production optimization experiments, media consisted of 25 mL Luria Broth (LB), Miller version (VWR Scientific), 50 μL of 25 mg/mL kanamycin (Sigma), and 50 μL of 0.5 mM NAD^+ (Sigma). The 4 flasks were inoculated with approximately 0.5 mL of a 5 mL overnight LB culture of *E. coli* BL21 DE3 containing pSD22 to 30 Klett (red filter) and grown at 37° and 225 rpm until a Klett reading of 75 was reached. At this point, the desired amount of isopropyl β- d-1-thiogalactopyranoside (IPTG, from Sigma) was added to a final concentration of: 0 mM, 0.2 mM, 0.6 mM, or 1 mM. Another 50 μL of NAD^+ was also added immediately to each flask after IPTG addition. After the addition of inducer, the flasks were grown at 37°C with shaking at 225 rpm. After 16 hours, the cultures were centrifuged at 11950 x g for 15 minutes at 4°C. Following the removal of the supernatant, the pellets were stored at -15°C. This process was then repeated later using temperatures of 25°C or 30°C after addition of IPTG.

3.1.2 Sonification

Cell pellets were resuspended in 2 mL of ice-cold 0.05 M potassium phosphate buffer (pH 7.5). They were then sonified on ice with a Branson Sonifier 450 fitted with a microtip for a total of 2 minutes (4 treatments of: 30 seconds on, 30 seconds off) and spun at 26890 x g for 25 minutes at 4°C. The supernatant was saved as a crude extract to immediately assay or purify.

3.2 Recombinant Urocanase Purification

3.2.1 Column Chromatography

Urocanase was purified from the crude extract using IMAC chromatography. For each crude extract derived from a 25 mL culture, a 1 mL nickel-charged IMAC column was prepared (BioRad). The column was first equilibrated with 0.05 M potassium phosphate (pH 7.5) containing 10% glycerol and 15 mM NAD^+. The crude extract was loaded onto the column, and then the column was washed with 2 column volumes (2 mL) of 0.05 M potassium phosphate (pH 7.5) buffer including 10 mM imidazole, 10% glycerol, and 15 mM NAD^+. This was followed by another wash with 6 column volumes (6 mL) of 0.05 M potassium phosphate (pH 7.5) with 30 mM imidazole, 10% glycerol, and 15 mM NAD^+. Urocanase was eluted from the column with 4 column volumes (4 mL) of 0.05 M potassium phosphate (pH 7.5), 200 mM imidazole, 10% glycerol, and 15 mM NAD^+. The column was later cleaned with 0.5 M imidazole and stored in 20% ethanol between uses; the entire column process was completed at 4°C.

3.2.2 Imidazole Removal

If using a 30 kDa spin filter (Amicon, 0.5 mL) to remove imidazole from column-purified enzyme samples, 0.5 mL of urocanase solution was added to the spin filter and centrifuged at maximum speed in an Eppendorf microfuge for 2.5 minutes, reducing the filter-retained volume to approximately 0.2 mL. More urocanase solution was added to bring the volume back up to 0.5 mL and the process was repeated until the entire urocanase column eluate solution (typically 4 mL total) was concentrated to a volume of 0.2 mL. Next, 0.05 M potassium phosphate buffer

(pH 7.5) with 10% glycerol and 15 mM NAD^+ was added to bring the volume up to 0.5 mL, and it was centrifuged for 2.5 minutes at top speed and 4°C. This was repeated 2 more times, and after the final spin, the contents were brought up to a final volume of 1 mL using the same buffer and stored at -20°C.

If using dialysis to remove imidazole instead of using a spin filter, 3 mL of the urocanase solution eluted off of the IMAC column was loaded into a Slide-A-Lyzer Dialysis Cassette (0.5 to 3 mL size, Thermo Fisher Scientific). The cassette was gently agitated in 500 mL of 0.05 M potassium phosphate buffer (pH 7.5) with 10% glycerol and 15 mM NAD^+ for 4 hours at 4°C. The contents of the cassette were removed and stored at -20°C.

3.2.3 Urocanase Assay

Urocanase activity was determined using a continuous spectrophotometric assay measuring the drop in absorbance at 277 nm as urocanate gets consumed. Absorbance readings at 277 nm were continuously taken over the course of at least 10 minutes to generate a constant slope. The slope of this line was the rate of change in OD per minute. This value was used along with a path length of 1 cm and a urocanate extinction coefficient of 18800 $M^{-1}cm^{-1}$ (Tabor & Mehler, 1955) in Beer's Law ($A=\varepsilon cl$) and followed with unit conversions, provided the units/mL of the urocanase sample assayed. The process of solving for urocanase activity could be reduced to the following formula: Urocanase activity (units/mL) = (change in OD/time)(dilution factor)(0.0532) where a unit is 1 μmole of urocanate consumed per minute under the assay conditions described here. Cuvettes consisted of 133 μL of 1 mM urocanate (pH 7.5), 266 μL of 0.05 M potassium phosphate buffer (pH 7.5), between 10 and 100 μL of sample appropriately

diluted in 0.05 M potassium phosphate buffer (pH 7.5), and distilled water up to 1 mL final volume.

3.2.4 Protein Determination

Total protein amount was determined using the Bradford Assay, which uses the binding of Coomassie Blue dye to proteins to create a complex that absorbs strongly at 595 nm (Bradford, 1976). A standard curve was made using bovine serum albumin (Sigma, No. A-4503). This was done in triplicate, and a second-degree polynomial regression line was fit to the data. To determine the concentration of protein in an unknown sample, 100 μL of properly diluted sample was added to 4 mL of assay reagent, vortexed, and incubated for 5 minutes at room temperature. The absorbance value at 595 nm was entered into the equation for the regression line generated for the standard curve to determine the concentration of protein.

3.2.5 Specific Activity Determination

Specific activity was determined using the following formula:

Specific Activity (Units/mg) = Activity (Units/mL) / Protein Concentration (mg/mL)

3.2.6 SDS-PAGE

Gels were cast in an SE215 Gel Caster (Hoefer). The 0.75 mm resolving gel (12% acrylamide, 0.6 M Tris (pH 8.8), 0.1% SDS, 0.1% ammonium persulfate, and 0.04% TEMED) was poured first. A thin layer of a water-saturated solution of butanol was laid over the top of the

resolving gel. After the resolving gel solidified, the butanol was removed, and the stacking gel (5% acrylamide, 0.125 M Tris (pH 6.8), 0.1% SDS, 0.1% ammonium persulfate, and 0.1% TEMED) was poured and a 10 well comb was inserted. Next, 5X loading dye (0.0625 M Tris-HCl, 10% glycerol, 2% SDS, 5% β-mercaptoethanol, and 0.00125% bromophenol blue) was added to the samples and boiled for 5 minutes. The gels were run in a SE250 Gel Electrophoresis Unit (Hoefer) using 0.025 M Tris (pH 8.3), 0.25 M glycine, 0.1% SDS running buffer. The gels were loaded with 15 μL of the ladder (Pre-Stained Protein Marker, Broad Range (7-175 kDa), NEB P7708s) and 15 μL of each prepared sample. The gel was run at 120 V for about 45 minutes, stained in Coomassie Blue dye for 2-3 hours, and then destained in 7% acetic acid and 5% methanol overnight. Destained gels were visualized with a lightbox.

3.3 Urocanase Cofactor Experiments

3.3.1 NAD^+ Analog Exchange

Urocanase was first purified using the previously described protocol section **3.2.1** with the following changes: a 50 mL culture was used along with a 2 mL IMAC column, all column buffers were made with sodium phosphate as the buffering agent, and the 30 mM imidazole column wash and 200 mM imidazole column wash did not contain NAD^+. The protein concentration was determined using the protocol detailed in section **3.2.4**. In each replicate, there was 225 μg of pure urocanase, a final concentration of 0, 4, 20, or 40 μM of NAD^+ or $NADP^+$, and enough 0.05 M sodium phosphate buffer pH (7.5), 10% glycerol for a final volume of 1 mL. Dilutions of 5 mM stock solutions at pH 7 were used to achieve the various concentrations of analog tested. The samples were frozen at -80°C for 24 hours. After freezing, the samples were

quickly thawed (less than 2 minutes) at 37°C and stored at 4°C while each replicate was assayed for activity using the urocanase assay described in section **3.2.3**. Specific activity of urocanase was then determined for each sample using the equation in section **3.2.5**. This was repeated for thio-NAD^+ and NHD^+ except 325 μg of urocanase was used, and the final concentrations of analog ranged from 0, 6, 30, and 60 μM.

3.4 Assay of Urocanase Activity While Bound to Agarose Beads

The desired amount of urocanase was added to nickel-charged IMAC resin suspended in 1 mL of buffer (0.05 M potassium phosphate (pH 7.5), with 10% glycerol and 15 μM NAD^+), mixed for 1 minute on a rotary clamp, and centrifuged for 30 seconds at max speed and room temperature, followed by the removal of excess liquid. To the tube, 267 μL of 0.05 potassium phosphate buffer (pH 7.5), 133 μL 1 mM urocanate solution (pH 7.5), and 600 μL of distilled water were added. Immediately after, a running clock was started, following which, the tube was inverted 5 times, rotated for 1 minute, and centrifuged for 30 seconds. A 50 μL aliquot was taken from the supernatant and boiled for 45 seconds, making sure that the time of extraction was recorded. This process was then repeated over the course of 10 minutes to gather at least 5 samples at different time points. After all of the samples were collected, they were diluted 1:4 with distilled water and the absorbance at 277 nm was taken. The absorbance of each aliquot was plotted with the time it was removed from the tube and fit with a linear regression model. The slope of this line was used to determine the activity of the urocanase using the same calculations as the standard urocanase assay described in section **3.2.3**. If free urocanase was assayed, the

tube contained the same contents of the bound urocanase tube without the addition of nickel agarose beads.

3.5 IoPA Synthesis

3.5.1 Enzyme-Mediated IoPA Synthesis

Synthesis of imidazolone propionate (IoPA) was done using a modified version of the procedure described by Brown and Kies (1959b) by scaling the reaction down and using immobilized instead of free urocanase. The reaction mixture contained 12.5 mL of 0.05 M potassium phosphate buffer (pH 7.5) and 0.5 mL of 1 M potassium urocanate (pH 7.5). The reaction flask was put in a vacuum oven set to 37°C and evacuated then flushed with nitrogen 3 times. A total of 3 units of urocanase on nickel agarose beads were quickly added to the flask, which was evacuated and flushed with nitrogen 3 more times. Aliquots of the flask were taken periodically and the absorbance at 277 nm was read. When the absorbance had dropped to 1% of its original level, the reaction was stopped with a brief centrifugation, removing the supernatant from the urocanase-bound beads. Hydrochloric acid, 1 mL of 4 N HCl, was added to the supernatant to stabilize the synthesized IoPA and prepare the sample for column chromatography.

3.5.2 IoPA Purification

After synthesis, the acidified reaction mixture was immediately loaded on a 23 x 1 cm Dowex 50-H+ (200 to 400 mesh) column equilibrated with 0.1 M HCl. After loading, the IoPA

was eluted off using 2 M HCl. Fractions of 5 mL were collected, and the absorbance at 230 and 260 nm for every other fraction was measured. A peak at 230 nm corresponded to the elution of IoPA, so these fractions were pooled and stored at -15°C. The concentration of IoPA was determined using the extinction coefficient of 4000 M^{-1} cm^{-1} determined by Brown & Kies (1959b).

3.6 α-KGM Synthesis

3.6.1 Enzyme-Mediated α-KGM Synthesis

Synthesis of α-ketoglutaramate (α-KGM) was done using a modified version of the procedure detailed by Hassall and Greenberg (1971). The reaction mixture contained 0.1 g of urocanate in 60 mL of 0.05 M potassium phosphate buffer (pH 7.5). The reaction flask was put in a vacuum oven set to 37°C and evacuated then flushed with nitrogen 3 times. A total of 3 units of urocanase on nickel agarose beads were quickly added to the flask, which was evacuated and flushed with nitrogen 3 more times. Aliquots of the flask were taken periodically and the absorbance at 277 nm was read. When the absorbance had dropped to 5% of its original level (approximately 3 hours), the reaction was stopped by brief centrifugation to remove the supernatant from the urocanase-bound beads. To aid in the breakdown of IoPA to α-KGM, 0.2 g of 2,6 dichlorophenolindophenol (DCPIP) was added to the reaction mixture and kept at 4°C until column purification was performed (no longer than 24 hours).

3.6.2 α-KGM Purification

To remove the DCPIP, the reaction mixture was loaded onto a 16 x 1.2 cm Dowex-1 X8 (200-400 mesh) column equilibrated in water. The α-KGM was eluted with 5 column volumes (approximately 125 mL) of 0.6 M acetic acid and neutralized to pH 7. In order to reduce the volume and increase the concentration of α-KGM, the eluent was lyophilized for 24 hours and resuspended in 4 mL of distilled water.

3.6.3 α-KGM Assay

Ketoacid content of the purified α-KGM was done using a modified version of an assay used by Krasnikov et al. (2009). An aliquot of 10 μL of α-KGM was added to 240 μL of 0.4 M Tris-HCl buffer (pH 8.0). To this, 100 μL of 5 mM 2,4-dinitrophenylhydrazine in 2 M HCl was added, and the mixture was left to incubate at room temperature for 5 minutes. To bring the pH up to around 10, 50 μL of 6 M NaOH was added along with 600 μL of distilled water for a final volume of 1 mL. The absorbance at 430 nm was taken and used in Beer's Law ($A=\varepsilon cl$) along with an extinction coefficient of 16,000 $M^{-1}cm^{-1}$ for the α-ketoglutarate-2,4 dinitrophenylhydrazone product to determine the concentration of α-KGM in the stock solution, which was 1.25 mM in this synthesis.

3.7 Aspartate Aminotransferase Assays

3.7.1 Aspartate Aminotransferase Assay with IoPA

Aspartate aminotransferase (AAT) was assayed by coupling the reaction to the reduction of oxaloacetate by malate dehydrogenase (MDH) using NADH:

Aspartate + α-ketoglutarate ⇌ glutamate + oxaloacetate (catalyzed by AAT)

Oxaloacetate + NADH + H^+ ⇌ malate + NAD^+ (catalyzed by MDH)

The decrease in absorbance at 340 nm was monitored which indirectly measured the rate of oxaloacetate produced by AAT by looking at NADH disappearance. Absorbance readings at 340 nm were continuously taken over the course of at least 10 minutes to generate a constant slope. The slope of this line was the rate of change in OD per minute. This value was used along with a path length of 1 cm and an extinction coefficient of 6220 $M^{-1}cm^{-1}$ in Beer's Law ($A=\varepsilon cl$) and followed with unit conversions, provided the units/mL of the AAT sample assayed.

Each cuvette contained 20 μL of crude extract from *E. coli* BL21 DE3, 13.5 μL of 13 mM NADH, 7.5 units of MDH, 2.25 μL of 444 mM α-ketoglutarate (pH 7.5), 800 μL of 0.1 M potassium phosphate buffer (pH 7.4) with 0.25 M aspartate, and 44.75 μL of either 2 M HCl or 4.2 mM purified IoPA neutralized with 106 μL of 1 M sodium bicarbonate. A cuvette with no α-ketoglutarate served as a control for background enzymatic activity in the crude extract that depleted NADH levels, and its activity was subtracted off of the tested samples. The protein concentration was determined using the method described in section **3.2.4** for each sample and using the AAT activity and protein amount, the specific activity for AAT was calculated.

3.7.2 Aspartate Aminotransferase Assay with α-KGM

AAT was assayed in a similar manner described in section **3.7.1**, except that α-KGM was used in place of IoPA. The cuvettes contained 20 μL of crude extract from *E. coli* BL21 DE3 cells, 13.5 μL of 13 mM NADH, 7.5 units of MDH, 9 μL of α-ketoglutarate (pH 7.5), 800 μL of 0.1 M potassium phosphate buffer (pH 7.4) with 0.25 M aspartate, and 144 μL of α-KGM. To test different α-ketoglutarate concentrations, the α-ketoglutarate was either diluted in water from a 444 mM stock solution to 55.6 mM (to test a final concentration of 0.5 mM), diluted to 111.1 mM (to test a final concentration of 1 mM), or undiluted (to test a final concentration of 4 mM). This way, the same volume of α-ketoglutarate could be used in each cuvette. Likewise, the 1.25 mM stock α-KGM solution was diluted in water to 0.14 mM, 0.35 mM, or 0.56 mM to test final concentrations of 0.02 mM, 0.05 mM, or 0.08 mM.

Chapter 4

Results: Expression and Purification of Urocanase

4.1 Sequencing of pSD22 Plasmid

Previous efforts in this laboratory by Kelly Helfrich and Steven Davis created the pSD22 plasmid that provides overexpression of an N-terminal 6-His-tagged urocanase gene product upon induction with IPTG. Site directed mutagenesis was used to introduce an NdeI site upstream of the *Pseudomonas putida hutU* start codon and a BamHI site at the end of the gene. This fragment was then cloned into a pET17b vector for overexpression of the urocanase gene, resulting in the pKH7 plasmid. To allow for immobilization of the enzyme, *hutU* from pKH7 was cut out and inserted into a pET28a vector that would add the N-terminal His-tag resulting in the final pSD22 vector. Details of this construction are found in the Methods and Materials section 3.0. This urocanase-containing vector (*hutU* from *P. putida* in pET28a) was then sequenced and found to be identical in nucleotide sequence following the NdeI site and continuing to the stop codon, with the sequence of urocanase from *P. putida* ATCC 12633 that had been determined in the laboratory (Fig. 1).

```
       ATTTTGTTTAACTTTAAGAAGGAGATATACCATGGGCAGCAGCCATCATCATCATCATCACAGCAGCGGCCTGGTGCCG
C 80
              |NdeI|
       GCGGCAGCCATATGACCGACAACAACAAATACCGTGACGTTGAAATCCGTGCCCCACGTGGCAACAAGCTGACCGCCAA
A 160

       AGCTGGCTGACCGAAGCGCCACTGCGCATGCTGATGAACAACCTCGACCCACAGGTTGCGGAAAACCCGAAAGAACTGG
T 240 GGTGTACGGCGGTATCGGCCGCGCCGCCCGCAACTGGGAATGCTACGATAAGATCGTCGAAACCCTGACCCGCCTGGAAG
320 ACGACGAAACCCTGCTGGTGCAGTCGGGCAAGCCGGTCGGCGTGTTCAAGACCCACAGCAATGCCCCGCGCGTGCTGATT
400 GCCAACTCCAACCTGGTGCCGCACTGGGCCAACTGGGAACACTTCAACGAACTGGACGCCAAAGGCCTGGCCATGTACGG
480 CCAGATGACCGCCGGCAGCTGGATCTACATCGGCAGCCAGGGCATCGTCCAGGGCACTTATGAAACCTTCGTCGAAGCCG
560 GTCGCCAGCACTACGGCGGCAGCCTGAAAGGCAAGTGGGTACTCACCGCAGGCCTCGGCGGCATGGGCGGCGCCCAGCCA
640 CTGGCTGCTACCCTGGCTGGCGCCTGCTCGCTGAACATCGAATGCCAGCAGAGCCGCATCGACTTCCGTCTGGAAACCCG
720 CTACGTCGACGAGCAGGCCACCGACCTCGACGACGCCCTGGTGCGCATCGCCAAATACACCGCCGAAGGCAAGGCCATCT
800 CCATCGCCCTGCACGGCAACGCTGCCGAAATCCTGCCAGAGCTGGTCAAGCGTGGCGTGCGCCCGGACATGGTCACCGAC
880 CAGACCAGCGCCCACGACCCGCTCAACGGCTACCTGCCTGCCGGCTGGACCTGGGAGCAGTACCGCGACCGCGCGCAGAC
960 CGAACCGGCTGCAGTGGTCAAGGCCGCCAAGCAGTCGATGGCCGTGCACGTGCAGGCCATGCTGGACTTCCAGAAGCAGG
1040 GCGTCCCGACCTTCGACTATGGCAACAACATCCGCCAGATGGCCAAGGAAGAGGGCGTGGCCAATGCCTTCGACTTCCCG
1120 GGCTTCGTCCCTGCCTATATCCGTCCGCTGTTCTGCCGCGGCGTAGGCCCTTTCCGCTGGGCGGCGCTGTCTGGCGAGGC
1200 CGAGGACATCTACAAGACCGACGCCAAGGTCAAGGAACTGATCCCCGACGACGCCCACCTGCACCGCTGGCTGGACATGG
1280 CCCGCGAGCGCATCAGCTTCCAGGGCCTGCCGGCACGTATCTGCTGGGTTGGCCTGGGCCTGCGCGCCAAGCTGGGCCTG
1360 GCCTTCAACGAAATGGTCCGCAGCGGCGAGCTGTCGGCACCGGTCGTGATCGGCCGTGACCACCTGGACTCGGGTTCGGT
1440 CTCCAGCCCCAACCGCGAAACCGAAGCCATGCGTGATGGCTCGGACGCTGTGTCCGACTGGCCGCTGCTCAACGCCCTGC
1520 TGAACACCGCAGGCGGCGCTACCTGGGTGTCGCTGCACCATGGTGGTGGCGTGGGCATGGGCTTCTCTCAGCACTCGGGC
1600 ATGGTCATCGTCTGCGACGGCACCGATGAAGCCGCCGAGCGCATCGCCCGTGTACTGACCAACGACCCAGGGACTGGCGT
1680 CATGCGCCACGCCGATGCCGGTTATGACATCGCCATCGACTGCGCCAAGGAGCAGGGCCTGGACCTGCCGATGATCACTG
1760 GCTGATTGCCACGCTTTGGATCC     1783
         STOP            BamHI

       # Location of the T7 promoter is approximately 40 base pairs upstream of the
sequence
       shown in the first line.  Details of this region are shown in a map of the pET-
28 vectors available from Novagen Corporation.
```

Figure 1. Plasmid pSD22 DNA sequence

The predicted amino acid sequence that should be found in the recombinant version of urocanase starting at the ATG codon present in the NcoI site (CCATGG) in pSD22 was determined (Fig. 2). The top line sequence contains the 6-His tag region and other amino acids added prior to the known sequence of *P. putida* urocanase. The second line begins with the NdeI sequence (CATATG) that contains the usual start codon position for urocanase, followed by the recognized amino acids that are present in this portion of the non-His tagged version of urocanase.

```
ccatgggcagcagccatcatcatcatcacagcagcggcctggtgccgcgcggcagc
   M  G  S  S  H  H  H  H  H  H  S  S  G  L  V  P  R  G  S

catatgaccgacaacaacaaataccgtgacgttgaaatccgtgcc ...
 H  M  T  D  N  N  K  Y  R  D  V  E  I  R  A
```

Figure 2. Predicted Amino Acid Sequence in the Recombinant Urocanase

The following data set contains BlastN results for the above DNA of pSD22, 1783 bp, as the Query sequence, versus the *hutCUH* gene sequence from our strain of *P. putida* ATCC 12633 as the subject (SBJCT). The two sequences match completely but only for bases shown between positions 93 and1782 bases (Fig. 3). This results from the fact that the Query sequence included the terminal BamHI GGATCC sequence but that sequence was created by SDM modification of a GGATCG sequence downstream of the *hutU* stop codon to become GGATCC in the SD22 plasmid. Thus, the last base comparison at position 1783 of pSD22 did not match the comparable sequence in the SBJCT (a G) and therefore the Blast result shows only 1690 bases (1782 minus 92) bases matched completely between pSD22 and the full DNA sequence. Sequence of the first 92 bases did not match known sequence for the *hutU* gene because positions 1 to 92 are bases only present in pET28a until the last 2 positions (TG) in the NdeI sequence were reached. All sequence that follows, starting at position 93, matched the known *hutU* DNA sequence until position 1783.

```
Query  93  TGACCGACAACAACAAATACCGTGACGTTGAAATCCGTGCCCCACGTGGCAACAAGCTGA 152
           ||||||||||||||||||||||||||||||||||||||||||||||||||||||||||||
Sbjct 2022 TGACCGACAACAACAAATACCGTGACGTTGAAATCCGTGCCCCACGTGGCAACAAGCTGA 2081

Query  153 CCGCCAAAAGCTGGCTGACCGAAGCGCCACTGCGCATGCTGATGAACAACCTCGACCCAC  212
           ||||||||||||||||||||||||||||||||||||||||||||||||||||||||||||
Sbjct 2082 CCGCCAAAAGCTGGCTGACCGAAGCGCCACTGCGCATGCTGATGAACAACCTCGACCCAC  2141

Query  213 AGGTTGCGGAAAACCCGAAAGAACTGGTGGTGTACGGCGGTATCGGCCGCGCCGCCCGCA  272
           ||||||||||||||||||||||||||||||||||||||||||||||||||||||||||||
Sbjct 2142 AGGTTGCGGAAAACCCGAAAGAACTGGTGGTGTACGGCGGTATCGGCCGCGCCGCCCGCA  2201
```

```
Query  273 ACTGGGAATGCTACGATAAGATCGTCGAAACCCTGACCCGCCTGGAAGACGACGAAACCC  332
           ||||||||||||||||||||||||||||||||||||||||||||||||||||||||||||
Sbjct 2202 ACTGGGAATGCTACGATAAGATCGTCGAAACCCTGACCCGCCTGGAAGACGACGAAACCC  2261

Query  333 TGCTGGTGCAGTCGGGCAAGCCGGTCGGCGTGTTCAAGACCCACAGCAATGCCCCGCGCG  392
           ||||||||||||||||||||||||||||||||||||||||||||||||||||||||||||
Sbjct 2262 TGCTGGTGCAGTCGGGCAAGCCGGTCGGCGTGTTCAAGACCCACAGCAATGCCCCGCGCG  2321

Query  393 TGCTGATTGCCAACTCCAACCTGGTGCCGCACTGGGCCAACTGGGAACACTTCAACGAAC  452
           ||||||||||||||||||||||||||||||||||||||||||||||||||||||||||||
Sbjct 2322 TGCTGATTGCCAACTCCAACCTGGTGCCGCACTGGGCCAACTGGGAACACTTCAACGAAC  2381

Query  453 TGGACGCCAAAGGCCTGGCCATGTACGGCCAGATGACCGCCGGCAGCTGGATCTACATCG  512
           ||||||||||||||||||||||||||||||||||||||||||||||||||||||||||||
Sbjct 2382 TGGACGCCAAAGGCCTGGCCATGTACGGCCAGATGACCGCCGGCAGCTGGATCTACATCG  2441

Query  513 GCAGCCAGGGCATCGTCCAGGGCACTTATGAAACCTTCGTCGAAGCCGGTCGCCAGCACT  572
           ||||||||||||||||||||||||||||||||||||||||||||||||||||||||||||
Sbjct 2442 GCAGCCAGGGCATCGTCCAGGGCACTTATGAAACCTTCGTCGAAGCCGGTCGCCAGCACT  2501

Query  573 ACGGCGGCAGCCTGAAAGGCAAGTGGGTACTCACCGCAGGCCTCGGCGGCATGGGCGGCG  632
           ||||||||||||||||||||||||||||||||||||||||||||||||||||||||||||
Sbjct 2502 ACGGCGGCAGCCTGAAAGGCAAGTGGGTACTCACCGCAGGCCTCGGCGGCATGGGCGGCG  2561

Query  633 CCCAGCCACTGGCTGCTACCCTGGCTGGCGCCTGCTCGCTGAACATCGAATGCCAGCAGA  692
           ||||||||||||||||||||||||||||||||||||||||||||||||||||||||||||
Sbjct 2562 CCCAGCCACTGGCTGCTACCCTGGCTGGCGCCTGCTCGCTGAACATCGAATGCCAGCAGA  2621

Query  693 GCCGCATCGACTTCCGTCTGGAAACCCGCTACGTCGACGAGCAGGCCACCGACCTCGACG  752
           ||||||||||||||||||||||||||||||||||||||||||||||||||||||||||||
Sbjct 2622 GCCGCATCGACTTCCGTCTGGAAACCCGCTACGTCGACGAGCAGGCCACCGACCTCGACG  2681

Query  753 ACGCCCTGGTGCGCATCGCCAAATACACCGCCGAAGGCAAGGCCATCTCCATCGCCCTGC  812
           ||||||||||||||||||||||||||||||||||||||||||||||||||||||||||||
Sbjct 2682 ACGCCCTGGTGCGCATCGCCAAATACACCGCCGAAGGCAAGGCCATCTCCATCGCCCTGC  2741

Query  813 ACGGCAACGCTGCCGAAATCCTGCCAGAGCTGGTCAAGCGTGGCGTGCGCCCGGACATGG  872
           ||||||||||||||||||||||||||||||||||||||||||||||||||||||||||||
Sbjct 2742 ACGGCAACGCTGCCGAAATCCTGCCAGAGCTGGTCAAGCGTGGCGTGCGCCCGGACATGG  2801

Query  873 TCACCGACCAGACCAGCGCCCACGACCCGCTCAACGGCTACCTGCCTGCCGGCTGGACCT  932
           ||||||||||||||||||||||||||||||||||||||||||||||||||||||||||||
Sbjct 2802 TCACCGACCAGACCAGCGCCCACGACCCGCTCAACGGCTACCTGCCTGCCGGCTGGACCT  2861

Query  933 GGGAGCAGTACCGCGACCGCGCGCAGACCGAACCGGCTGCAGTGGTCAAGGCCGCCAAGC  992
           ||||||||||||||||||||||||||||||||||||||||||||||||||||||||||||
Sbjct 2862 GGGAGCAGTACCGCGACCGCGCGCAGACCGAACCGGCTGCAGTGGTCAAGGCCGCCAAGC  2921

Query  993 AGTCGATGGCCGTGCACGTGCAGGCCATGCTGGACTTCCAGAAGCAGGGCGTCCCGACCT  1052
           ||||||||||||||||||||||||||||||||||||||||||||||||||||||||||||
Sbjct 2922 AGTCGATGGCCGTGCACGTGCAGGCCATGCTGGACTTCCAGAAGCAGGGCGTCCCGACCT  2981

Query 1053 TCGACTATGGCAACAACATCCGCCAGATGGCCAAGGAAGAGGGCGTGGCCAATGCCTTCG  1112
           ||||||||||||||||||||||||||||||||||||||||||||||||||||||||||||
Sbjct 2982 TCGACTATGGCAACAACATCCGCCAGATGGCCAAGGAAGAGGGCGTGGCCAATGCCTTCG  3041
```

```
Query 1113 ACTTCCCGGGCTTCGTCCCTGCCTATATCCGTCCGCTGTTCTGCCGCGGCGTAGGCCCTT  1172
           ||||||||||||||||||||||||||||||||||||||||||||||||||||||||||||
Sbjct 3042 ACTTCCCGGGCTTCGTCCCTGCCTATATCCGTCCGCTGTTCTGCCGCGGCGTAGGCCCTT  3101

Query 1173 TCCGCTGGGCGGCGCTGTCTGGCGAGGCCGAGGACATCTACAAGACCGACGCCAAGGTCA  1232
           ||||||||||||||||||||||||||||||||||||||||||||||||||||||||||||
Sbjct 3102 TCCGCTGGGCGGCGCTGTCTGGCGAGGCCGAGGACATCTACAAGACCGACGCCAAGGTCA  3161

Query 1233 AGGAACTGATCCCCGACGACGCCCACCTGCACCGCTGGCTGGACATGGCCCGCGAGCGCA  1292
           ||||||||||||||||||||||||||||||||||||||||||||||||||||||||||||
Sbjct 3162 AGGAACTGATCCCCGACGACGCCCACCTGCACCGCTGGCTGGACATGGCCCGCGAGCGCA  3221

Query 1293 TCAGCTTCCAGGGCCTGCCGGCACGTATCTGCTGGGTTGGCCTGGGCCTGCGCGCCAAGC  1352
           ||||||||||||||||||||||||||||||||||||||||||||||||||||||||||||
Sbjct 3222 TCAGCTTCCAGGGCCTGCCGGCACGTATCTGCTGGGTTGGCCTGGGCCTGCGCGCCAAGC  3281

Query 1353 TGGGCCTGGCCTTCAACGAAATGGTCCGCAGCGGCGAGCTGTCGGCACCGGTCGTGATCG  1412
           ||||||||||||||||||||||||||||||||||||||||||||||||||||||||||||
Sbjct 3282 TGGGCCTGGCCTTCAACGAAATGGTCCGCAGCGGCGAGCTGTCGGCACCGGTCGTGATCG  3341

Query 1413 GCCGTGACCACCTGGACTCGGGTTCGGTCTCCAGCCCCAACCGCGAAACCGAAGCCATGC  1472
           ||||||||||||||||||||||||||||||||||||||||||||||||||||||||||||
Sbjct 3342 GCCGTGACCACCTGGACTCGGGTTCGGTCTCCAGCCCCAACCGCGAAACCGAAGCCATGC  3401

Query 1473 GTGATGGCTCGGACGCTGTGTCCGACTGGCCGCTGCTCAACGCCCTGCTGAACACCGCAG  1532
           ||||||||||||||||||||||||||||||||||||||||||||||||||||||||||||
Sbjct 3402 GTGATGGCTCGGACGCTGTGTCCGACTGGCCGCTGCTCAACGCCCTGCTGAACACCGCAG  3461

Query 1533 GCGGCGCTACCTGGGTGTCGCTGCACCATGGTGGTGGCGTGGGCATGGGCTTCTCTCAGC  1592
           ||||||||||||||||||||||||||||||||||||||||||||||||||||||||||||
Sbjct 3462 GCGGCGCTACCTGGGTGTCGCTGCACCATGGTGGTGGCGTGGGCATGGGCTTCTCTCAGC  3521

Query 1593 ACTCGGGCATGGTCATCGTCTGCGACGGCACCGATGAAGCCGCCGAGCGCATCGCCCGTG  1652
           ||||||||||||||||||||||||||||||||||||||||||||||||||||||||||||
Sbjct 3522 ACTCGGGCATGGTCATCGTCTGCGACGGCACCGATGAAGCCGCCGAGCGCATCGCCCGTG  3581

Query 1653 TACTGACCAACGACCCAGGGACTGGCGTCATGCGCCACGCCGATGCCGGTTATGACATCG  1712
           ||||||||||||||||||||||||||||||||||||||||||||||||||||||||||||
Sbjct 3582 TACTGACCAACGACCCAGGGACTGGCGTCATGCGCCACGCCGATGCCGGTTATGACATCG  3641

Query 1713 CCATCGACTGCGCCAAGGAGCAGGGCCTGGACCTGCCGATGATCACTGGCTGATTGCCAC  1772
           ||||||||||||||||||||||||||||||||||||||||||||||||||||||||||||
Sbjct 3642 CCATCGACTGCGCCAAGGAGCAGGGCCTGGACCTGCCGATGATCACTGGCTGATTGCCAC  3701

Query 1773 GCTTTGGATC  1782
           ||||||||||
Sbjct 3702 GCTTTGGATC  3711
```

Query = pSD22 full sequence

Sbjct = genes CUH sequence from PSU P. putida strain ATCC 12633

Figure 3. BlastN Results for pSD22 DNA Urocanase Sequence

Differences were noted when comparing DNA sequences for pSD22 and the GenBank Accession # X58483.1 which is the DNA sequence for *Pseudomonas putida* urocanase reported by a German group (Fig. 4). These differences are also seen when that GenBank sequence was matched against our laboratory's complete sequence of *hutU* DNA as determined previously here. These are apparent differences due minor variations in the two *P. putida* strains. The extent of these differences are changes in 4 bases that result in 3 conservative amino acid changes, likely with little or no impact on the functionality of either urocanase.

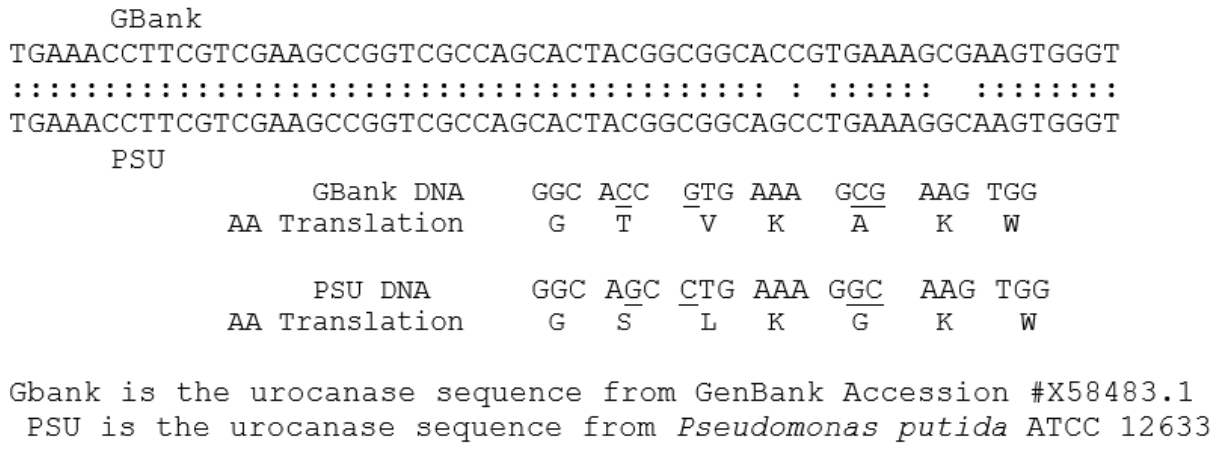

Figure 4. Comparison of Four Base Differences in Two Urocanase DNA Sequences

4.2 Optimization of Urocanase Expression

The pSD22 plasmid was transformed into the Bl21 DE3 strain of *E. coli* to allow for protein overexpression and simple purification. Because of the use of a pET28 vector as the backbone, protein expression was induced using IPTG, a lactose analog, that would activate the lac operon controlling the *hutU* gene. In order to get sufficient urocanase production from the cells, both the growing temperature and inducer concentration were optimized. Four concentrations of IPTG were tested (0, 0.2, 0.6, and 1 mM), and after addition of inducers, three

growing temperatures were studied (25, 30, and 37℃). A growing temperature of 25℃ was chosen to be the best because it had a higher specific activity for urocanase in the crude extract compared to the other temperatures (Fig. 5). Because the specific activity values were very similar between 0.2, 0.6, and 1 mM IPTG, an inducer concentration of 0.2 mM was chosen to move forward with because there was more total protein produced (Fig. 6). The total protein data in Fig. 6 was used to calculate the specific activity values shown in Fig. 5, but total protein is displayed separately here because it was also a factor in choosing growing conditions that promoted high levels of urocanase production.

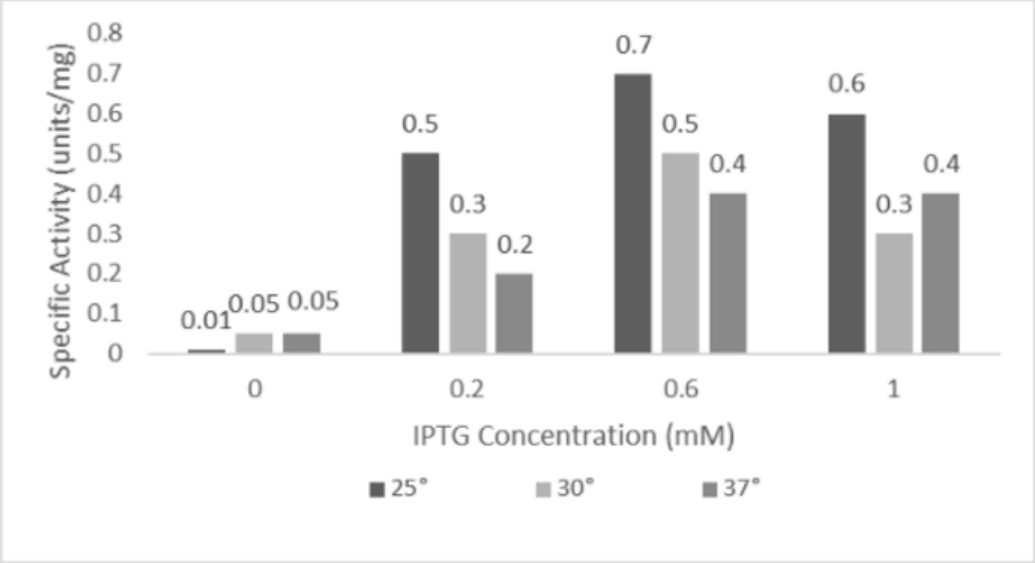

Figure 5. Specific activity of Urocanase in Cultures Containing pSD22

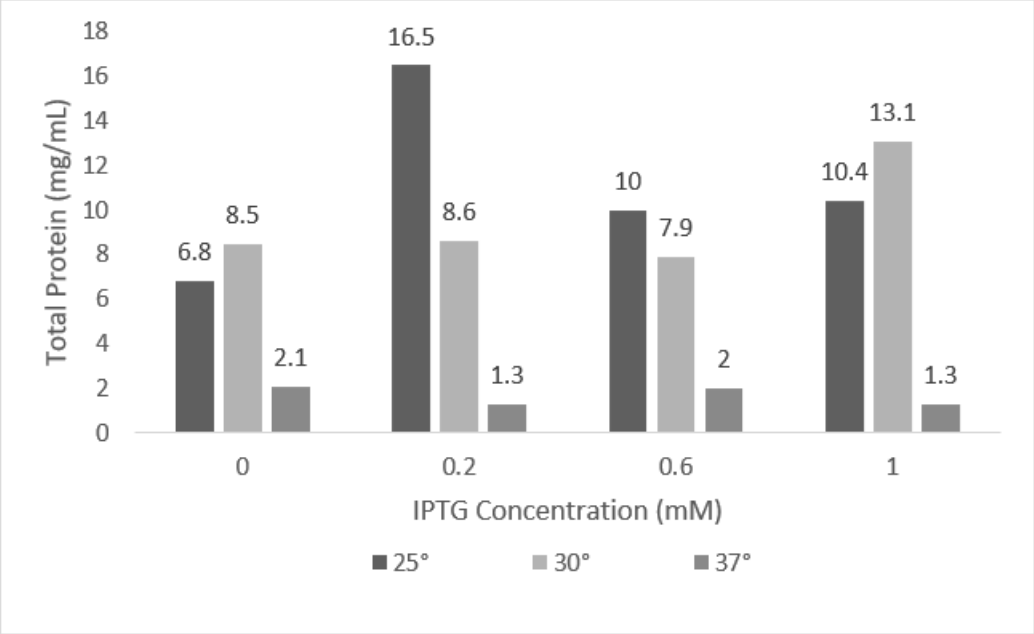

Figure 6. Total Protein in Cultures Containing pSD22

4.3 Optimization of Urocanase Purification

Purification of urocanase from the crude extract was accomplished with a one-step process using a nickel-charged IMAC column. SDS-PAGE analysis showed a smear of proteins in lane 2 for the crude extract and a single band in lane 6 for the purified urocanase sample around 58 kDa, which is close to the expected monomeric size of 60 kDa (Fig. 7). The composition of each of the column fractions are also shown, where lanes 3 and 4 correspond to the proteins from the crude extract that do not bind to column, and lane 5 shows the loosely-bound proteins that are washed off with a moderate amount of imidazole. Because of the lack of contaminating proteins seen in lane 6 of the gel, which contains the eluted urocanase, the one-step IMAC purification was deemed sufficient for purifying urocanase.

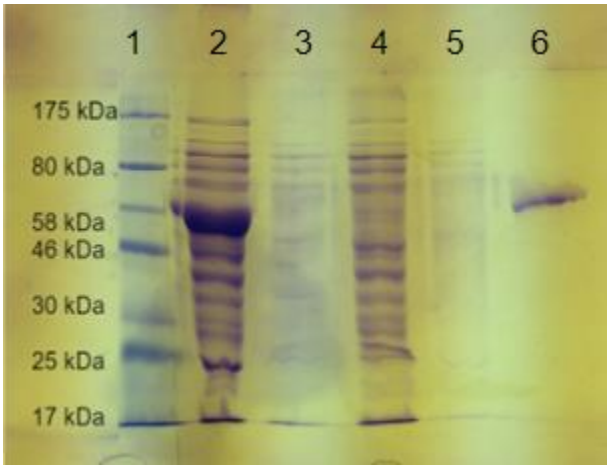

Figure 7. SDS-PAGE Analysis of Urocanase Purification

Lane 1: ladder, Lane 2: crude extract, Lane 3: flow-through after loading crude extract, Lane 4: 10 mM imidazole wash, Lane 5: 30 mM imidazole wash, Lane 6: 200 mM imidazole wash. 20 µL of each sample was loaded.

While the purification procedure resulted in easily obtained, pure urocanase, there were initial issues with retaining enzymatic activity throughout the procedure. Initial purification protocols resulted in a low yield of 12%. In an attempt to address this issue by optimizing the buffer conditions throughout the purification, the column wash buffers were made with 15mM NAD^+, the cofactor for urocanase. This change brought the yield up to 46%, a marked increase from previous attempts (Table 1). While a higher recovery would have been ideal, these conditions were chosen for future purifications in order to advance to more interesting experiments.

Table 1. Purification Scheme for Recombinant Urocanase

Fraction	Volume (mL)	Total Protein (mg)	Total Activity (units)	Specific Activity (U/mg)	Fold	Yield (%)
Crude Extract	4.2	7.6	7.6	1	1	100
Ni-NTA Column	3.9	1.6	3.5	2.2	2.2	46

4.4 Removal of Imidazole from Purified Urocanase Preparations

For many enzymes, it has been shown that the presence of imidazole can inhibit enzymatic activity, so it was initially of interest to reduce the concentration of imidazole present in the final eluent. However, doing so resulted in a substantial loss in specific activity when comparing the activity of the enzyme coming off the column to its activity after treatment to remove imidazole (Table 2). Multiple methods of removal were attempted, but the decrease in specific activity was still seen. Factors such as stability issues due to the length of the procedure were eliminated as a cause for the drop in activity using control experiments not shown here. Because the specific activity was the highest in fractions of urocanase coming off the column with no other treatment, these fractions were used for subsequent experiments.

Table 2. Specific Activity of Urocanase in the Presence of Imidazole

Method to Remove Imidazole	Specific Activity Immediately After Purification (units/mg)	Specific Activity After Removing Imidazole (units/mg)
None	2.2	NA
30 kDa Spin Filter	2	0.8
Dialysis	3.3	2

Chapter 5

Results: Cofactor Analysis of Urocanase

Because urocanase utilizes its cofactor NAD^+ in a unique way as an electrophile instead of an oxidizing agent, it was of interest to see whether analogs of NAD^+ would behave in a similar manner in this uncommon chemical role. Due to the tight interaction between urocanase and NAD^+, a system utilizing the slight change in pH of sodium phosphate buffer upon freezing was used. As the dibasic sodium phosphate falls out of solution due to decreased solubility, the pH drops enough that the conformation of urocanase shifts to release the bound NAD^+ without full denaturation. In the presence of excess analog capable of binding to an unoccupied NAD^+ site, the refolding urocanase takes up the analog upon thawing.

5.1 Optimization of Purification Buffers for Cofactor Exchange Experiments

Because this experiment requires a minimal amount of unbound (free) NAD^+ present in the purified urocanase sample so that the amount of NAD^+ or analog subsequently added is essentially the total amount present, the urocanase purification protocol had to be reworked. The four initially optimized purification buffers (0.05 M potassium phosphate buffer (pH 7.5), with 10% glycerol, 15 μM NAD^+, and either 0, 10, 30, or 200 mM imidazole) all contained the NAD^+ to improve the urocanase recovery. Simply removing NAD^+ from all the buffers would result in a final enzyme solution with too low of a specific activity to use for the cofactor analog studies. To determine the best combination of buffers to use to compromise between low amounts of NAD^+ in the final elution and high specific activity, NAD^+ was systematically removed from

different column washes and the final specific activities were compared. All purifications performed for the analog studies were done with 15 μM NAD^+ present in only the 0 mM and 10 mM imidazole-containing purification buffers but not the 30 mM and 200 mM imidazole purification buffers.

5.2 Nicotinamide Adenine Dinucleotide Phosphate Exchange

To establish the system of testing, nicotinamide adenine dinucleotide phosphate ($NADP^+$) was chosen as an expected negative control. It has not been identified as a cofactor of urocanase in any previous literature, and does not seem to naturally bind. This fits the general trend that most enzymes can either use NAD^+ or $NADP^+$, but not both. Using the same purified urocanase mixture, a series of trials were set up that had 225 μg of urocanase and varying amounts of NAD^+ or $NADP^+$. Each sample was frozen at -80°C for 24 hours to ensure enough time for the urocanase to unfold slightly and exchange the bound NAD^+ for the analog present in the solution upon freezing. The specific activity of each sample was then found after thawing at 37°C (Table 3). Three replicates were tested for each condition, and the mean and standard deviation are reported here.

If the urocanase was frozen without any NAD^+ present in the buffer, low activity was observed. Without added NAD^+ in the buffer, upon thawing, the concentration of NAD^+ was too low for the urocanase to rebind a new molecule of NAD^+ to make up for the NAD^+ lost during freezing. The presence of 4 μM NAD^+ was not enough to restore activity, but 20 μM increased the activity a substantial amount. The addition of any amount of $NADP^+$ did not restore the

specific activity of urocanase to the level that 20 μM of NAD^+ did. Because a restoration in activity was not observed, the $NADP^+$ was unable to be used catalytically by urocanase.

Table 3. Nicotinamide Adenine Dinucleotide Phosphate Exchange

	No NAD^+	4 μM NAD^+	20 μM NAD^+	4 μM $NADP^+$	20 μM $NADP^+$	40 μM $NADP^+$
Specific Activity (units/mg)	0.9 ± 0.1	1.3 ± 0.1	2.4 ± 0.9	0.9 ± 1.1	1.2 ± 0.7	0.4 ± 0.1

5.3 Thionicotinamide Adenine Dinucleotide Exchange

After observing the non-functional outcome for $NADP^+$, thionicotinamide adenine dinucleotide (thio-NAD^+) was then tested in a slightly modified fashion (Table 4). For its evaluation with urocanase, the concentrations of this analog were compared with equal amounts of NAD^+ and a constant amount of urocanase (325 μg), an increase over the amount used in Table 3. Similar to the first trial done with $NADP^+$, addition of no NAD^+ resulted in low activity after freezing. Small amounts of NAD^+ (6 μM) were not enough to restore enzyme activity, but the addition of 30 μM NAD^+ led to full recovery. The addition of thio-NAD^+ did not increase the activity of urocanase to the level seen with addition of 30 μM NAD^+, indicating that it cannot be used for catalysis by urocanase.

Table 4. Thionicotinamide Adenine Dinucleotide Exchange

	No NAD^+	6 μM NAD^+	30 μM NAD^+	6 μM Thio-NAD^+	30 μM Thio-NAD^+	60 μM Thio-NAD^+
Specific Activity (units/mg)	0.9 ± 0.2	1.0 ± 0.4	2.7 ± 0.7	1.2 ± 0.4	1.7 ± 0.7	0.9 ± 0.1

5.4 Nicotinamide Hypoxanthine Dinucleotide Exchange

Thio-NAD^+ has an altered nicotinamide moiety, which is the catalytically relevant end of NAD^+. It was also of interest to look at an analog that has the nucleotide moiety chemically altered, which would likely have less of an impact on urocanase activity. To study this, nicotinamide hypoxanthine dinucleotide (NHD^+) was used as the experimental analog in a study set up similarly to the Thio-NAD^+ trial using 325 μg of urocanase (Table 5). In this case, 30 or 60 μM of NHD^+ restored specific activity to levels comparable to 30 μM of NAD^+. The recovery of urocanase activity indicates the potential for NHD^+ to be used for catalysis by urocanase.

Table 5. Nicotinamide Hypoxanthine Dinucleotide Exchange

	No NAD^+	6 μM NAD^+	30 μM NAD^+	6 μM NHD^+	30 μM NHD^+	60 μM NHD^+
Specific Activity (units/mg)	2.8 ± 0.1	2.6 ± 0.2	3.8 ± 0.5	3.3 ± 0.2	3.7 ± 0.5	3.5 ± 0.4

Chapter 6

Results: IoPA and α-KGM Synthesis

In order to study the potentially inhibitory effects of breakdown products of IoPA, both IoPA and the breakdown product of interest, α-ketoglutaramate (α-KGM), needed to be synthesized. To avoid having to carry out a chemical synthesis, an enzymatic route was taken using immobilized urocanase. The recombinant his-tagged urocanase expressed from the pSD22 plasmid was purified and then re-immobilized on nickel-charged IMAC beads. The immobilized enzyme was then used to make IoPA and α-KGM by adding urocanate, stopping the reaction by removing the enzyme-bound beads, and then purifying the desired compound.

6.1 Bound Urocanase Assay

Before the syntheses could take place, the activity of urocanase on the beads was verified to ensure that catalysis could still happen efficiently in the immobilized state. Because the IMAC beads could not be used for the standard spectrophotometric assay for urocanase, a variation of the assay was developed. Purified urocanase was immobilized on a small amount of nickel-charged beads, to which an assay reagent containing urocanate was added. Periodically, the beads were centrifuged to the bottom of the tube and an aliquot of the supernatant was removed. The aliquot was boiled to prevent further urocanase activity, and absorbance readings were taken to determine the amount of urocanate left. The absorbance values were graphed against time to

get the change in absorbance per minute, which could then be converted to units of enzymatic activity (Fig. 8). This was done for both free and immobilized urocanase, and it was found that the free urocanase had a specific activity of 1.4 units/mg and the immobilized urocanase had a specific activity of 0.8 units/mg. This meant that 1 unit of free urocanase corresponded to 0.6 units of activity when immobilized.

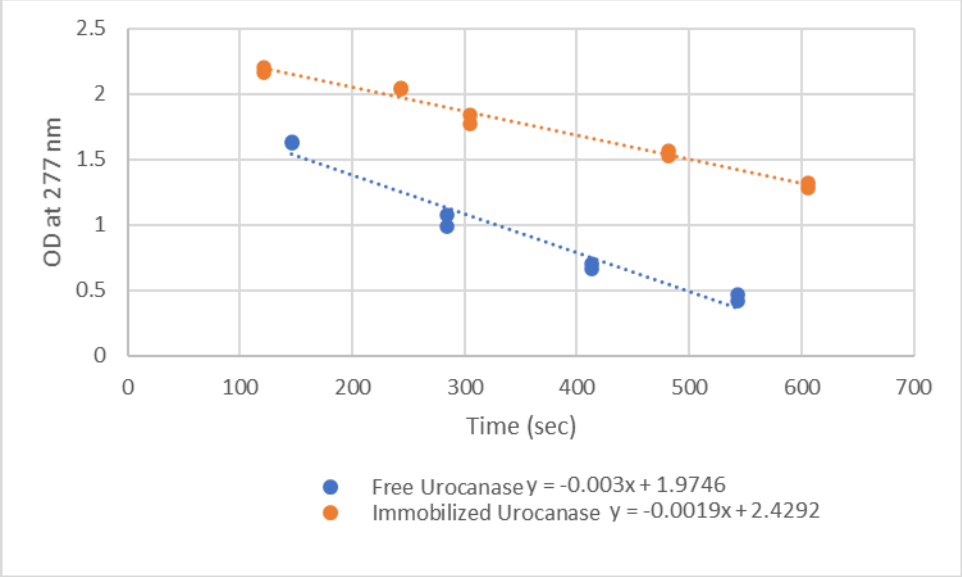

Figure 8. Bound Urocanase Assay

Change in absorbance at 277 nm for free and immobilized urocanase using the immobilized urocanase assay. 7 µg of purified urocanase was used to prepare the immobilized enzyme or as free enzyme for each assay. The slope of each line of best fit was used to calculate the activity of urocanase using the same calculations as the standard urocanase assay.

6.2 IoPA Synthesis

Using the immobilized urocanase, IoPA was synthesized as described in section **3.5.1** and purified using the method detailed in section **3.5.2**. IoPA absorbs strongly at 230 nm and urocanate absorbs strongly at 260 nm, so the absorbance readings at these wavelengths were used to follow their respective compounds (Fig. 9). The large peak that occurred at 230 nm

between 100 and 200 mL corresponded to IoPA, which elutes off the column before urocanate. The smaller peak in readings at 260 nm from 300 to 350 mL was the residual urocanate that was not consumed during the reaction. The fractions included in the peak for IoPA were pooled together for a final concentration of 2.3 mM. Given the combined volume of the fractions and the concentration of the sample, a total of 0.13 millimoles of IoPA was recovered. The purity of the pooled fractions was confirmed with an absorbance spectrum (Fig. 10) that followed expected trends seen in Brown & Kies, (1959b).

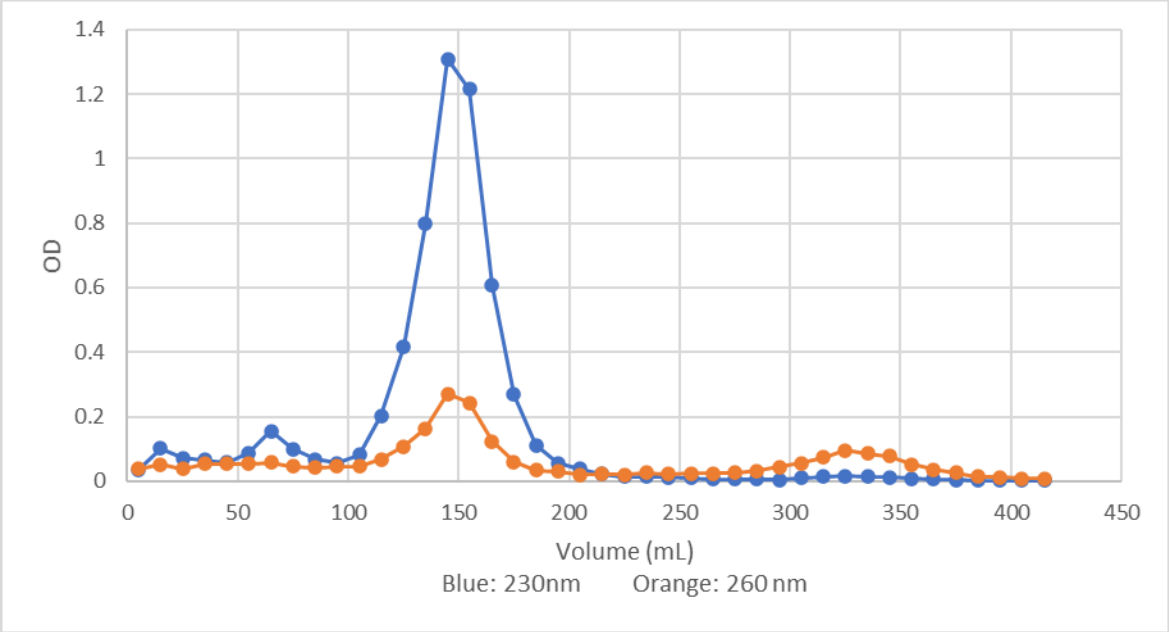

Figure 9. Elution curve of IoPA

Following IoPA and urocanate after separation on a Dowex 50 column using 2 M HCl to elute. Peaks of absorbance at 230 nm correspond to IoPA elution and peaks at 260 nm correspond to urocanate.

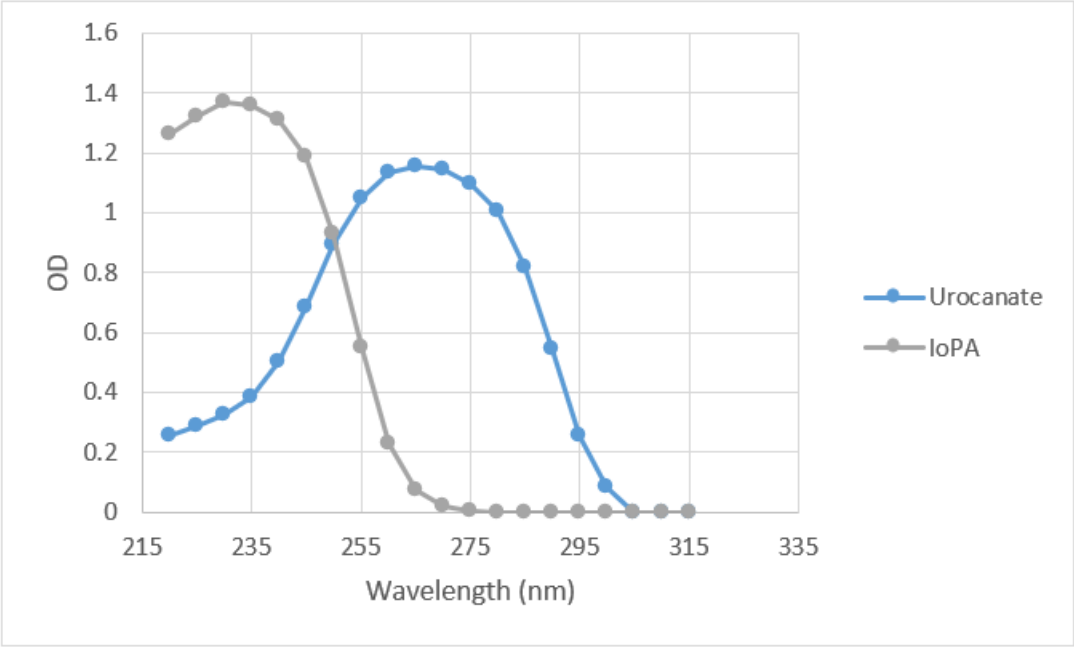

Figure 10. Absorbance spectrum of Purified IoPA

Cuvettes contained either 0.1 mM urocanate or 0.07 mM IoPA in 2 M HCl.

6.3 α-KGM Synthesis

Similar to IoPA, α-KGM was also synthesized with immobilized urocanase as described in section **3.6**. Because of background noise from acetic acid, spectrophotometric methods of following α-KGM content at 233 nM were not able to be used. Instead, a colorimetric assay was employed that relied on the reaction between 2,4-dinitrophenylhydrazine and a ketone. Assaying the final solution after synthesis, column chromatography, and lyophilization gave an α-KGM concentration of 1.25 mM. With a total volume of 4 mL, there was a total of 0.005 millimoles of α-KGM recovered.

Chapter 7

Results: Inhibition of AAT

7.1 Effect of IoPA on AAT

Based on previous work discussed in section **2.3**, the proposed mechanism of IoPA-related growth reduction was inhibition of aspartate aminotransferase (AAT). In order to study this potential interaction, AAT was assayed in the presence of the synthesized IoPA and α-KGM. Due to the requirement of oxygen for observed growth inhibition to aid in the degradation of IoPA, IoPA itself is likely not the inhibitory compound. To confirm this, AAT from *E. coli* crude extract was assayed in the presence of IoPA immediately after being neutralized (Table 6). This was done in triplicate, and the mean and standard deviation are reported here. IoPA is stable in acid, so by assaying immediately following its neutralization, there was not enough time for breakdown products to build up in significant amounts. There was essentially no change in AAT activity observed, supporting the hypothesis that IoPA itself does not inhibit AAT.

Table 6. AAT Activity in the Presence of IoPA

	No IoPA	0.2 mM IoPA
Specific Activity (Units/mg)	0.17 ± 0.01	0.15 ± 0.02

7.2 Effect of α-KGM on AAT

Since IoPA itself did not inhibit AAT, one of its breakdown products (α-KGM) was purified and used in similar assays to see if that compound had an inhibitory effect. Indeed, increasing amounts of α-KGM resulted in a corresponding decrease in AAT activity (Table 7). Each concentration of α-KGM was tested in triplicate with the mean and standard deviation reported here. Adding up to 0.2 mM of α-KGM caused an 8-fold decrease in AAT activity. Compared to adding the same amount of IoPA, α-KGM caused a notably higher reduction in AAT activity, indicating that it is α-KGM, not IoPA, that is the inhibitory molecule.

Table 7. AAT Activity in the Presence of α-KGM

α-KGM concentration (mM)	0	0.02	0.1	0.2
AAT specific activity (units/mg)	0.16 ± 0.01	0.12 ± 0.007	0.062 ± 0	0.024 ± 0.006

7.3 Type of α-KGM Inhibition

Due to the structural similarities with α-ketoglutarate, one of the substrates for AAT, α-KGM was predicted to be a competitive inhibitor. In order to determine if this was in fact the case, a Lineweaver-Burk plot was constructed using AAT velocities at varying α-ketoglutarate and α-KGM concentrations (Fig. 11). A linear regression line was then fit to each set of

velocities at a given α-KGM concentration. Visual analysis of the plot shows that the line for each inhibitor concentration roughly intersects at the Y-axis, which indicates competitive inhibition.

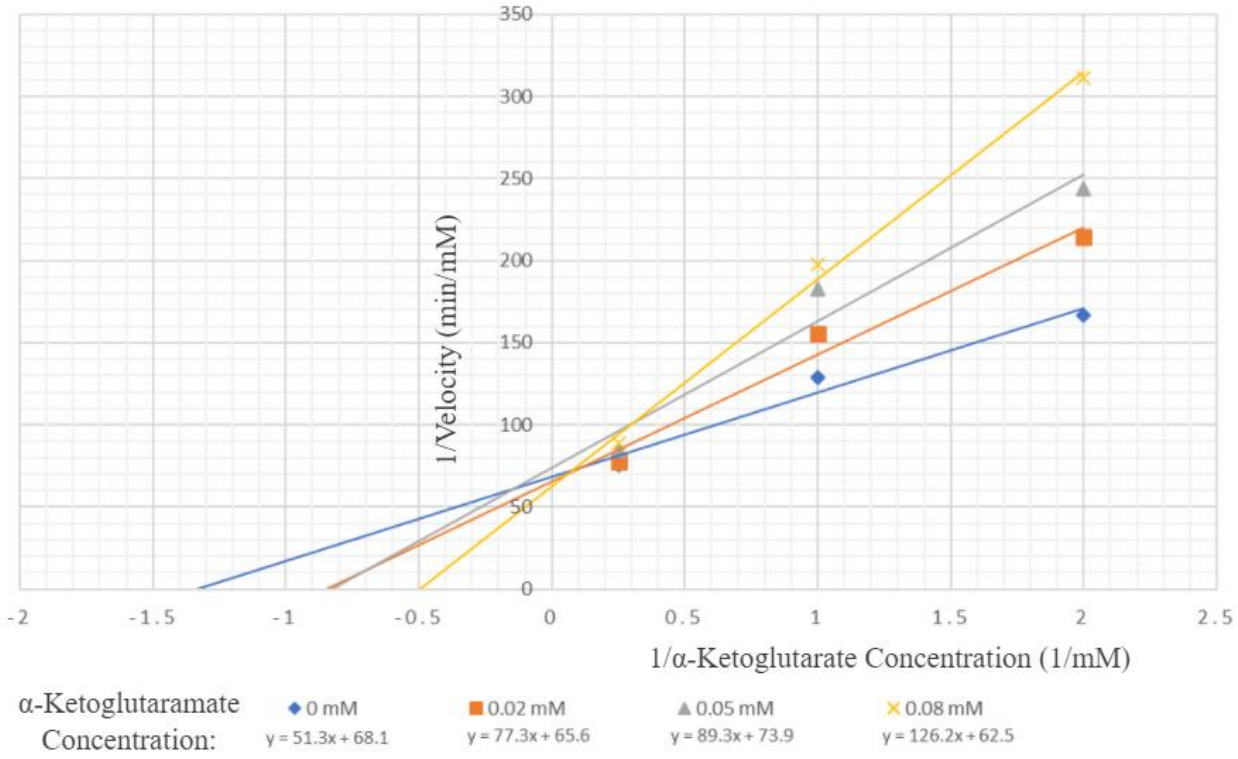

Figure 11. Lineweaver-Burk Plot of AAT Activity in the Presence of α-KGM

Using the equation of the regression line, the V_{max} and K_M were found for each condition (Table 8). As the concentration of α-KGM increased, the V_{max} stayed the same but the apparent K_M (K_{Mapp}), which is dependent upon the concentration of inhibitor, increased. This is characteristic of competitive inhibitors, as high concentrations of the natural substrate can relieve the effects of inhibition by outcompeting the inhibitor for the active site. This results in a conservation of the enzyme's maximal velocity, or V_{max}. However, the K_{Mapp} increased,

indicating decreased affinity for the natural substrate as the inhibitor competes for active site binding. Additionally, the linear regression line was used to find K_I, which came out to 0.05 ± 0.02 mM.

Table 8. Vmax and K_M or K_{Mapp} of AAT in the Presence of α-KGM

Concentration of α-KGM (mM)	0	0.02	0.05	0.08
V_{max} (mM/min)	0.015	0.015	0.014	0.016
K_M or K_{Mapp}(mM)	0.75 (K_M)	1.2 (K_{Mapp})	1.2 (K_{Mapp})	2.0 (K_{Mapp})

Chapter 8

Discussion

8.1 Expression and Purification of Urocanase

Through expression studies and purification optimization, the specific activity of recombinant His-tagged urocanase was comparable to the reported values for native urocanase (Egan et al., 1981). Since the addition of the tag has not been shown to significantly alter catalytic activity, the His-tagged version of urocanase then becomes a powerful tool to be able to easily purify large amounts of protein. However, the purification protocol still leaves room for further optimization. While the yield was brought up four-fold from the initial attempts, it still only sits just below 50%. Significantly scaling up the procedure could minimize the effects of low yield by starting with more urocanase in the crude extract to be purified, but scaling provides its own challenges as well.

In addition, previous studies have shown that urocanase specific activity can be brought even higher through photoactivation (Klepp & Retey, 1989). Irradiation at 320 nm is thought to eliminate the occasionally found inactive adduct formed between NAD^+ and the enzyme, thus increasing the activity of urocanase by allowing for the correct binding of NAD^+ (Klepp & Retey, 1989). Photoactivation was attempted here but was unsuccessful, likely due to having to use a UV lamp emitting a range of wavelengths instead of just one wavelength at 320 nm. Revisiting this idea with the correct equipment could increase the yield of urocanase obtained in the purification.

While the recombinant urocanase did not show differences in catalytic activity, it displayed signs of decreased stability because of the ease at which it could lose NAD^+. Previous

characterizations of natural urocanase showed that it binds NAD^+ extremely tightly and does not lose it through dialysis (Egan & Phillips, 1977). The recovery of activity seen when adding NAD^+ to the purification buffers for the His-tagged recombinant urocanase indicates that it lost its NAD^+ at some point in the purification process. Exploring the affinity of the His-tagged urocanase for NAD^+ compared to purified native enzyme would give insight on whether the addition of a His tag affected the ability of urocanase to bind NAD^+.

8.2 Urocanase Cofactor Specificity

The recombinant urocanase allowed for the purification of sufficient amounts of urocanase to be used for studies on the specificity of urocanase for its cofactor, NAD^+. Through these experiments it was shown that NHD^+ could be used just as well as NAD^+. Although thio-NAD^+ can be used by enzymes like alcohol and glutamate dehydrogenase (Biellmann et al., 1974), urocanase was not able to do so. This indicates that in the unique chemical environment that urocanase presents, alterations in the nicotinamide moiety have a more devastating effect; NHD^+ could be used without issue, but thio-NAD^+ could not. Exploring other analogs that also have chemical modifications in the nicotinamide ring would give further insight, such as acetylpyridine adenine dinucleotide.

In addition, it would be of value to confirm that the system of replacing analogs used here works. Expected decreases in activity were seen when either adding no NAD^+ or adding $NADP^+$, a negative control, in the sodium phosphate freezing method used. Verification using a labeled analog of NAD^+ would further support this experimental system and the results obtained. Use of labeled NAD^+ would also address the issue that the current experimental system does not show

how much of the added analog actually binds to the enzyme. A negative result could mean that the analog is unable to bind or that it can bind but is not catalytically active. Alternatively, other methods of slightly denaturing proteins could be explored, such as the use of ammonium sulfate to try to swap the tightly bound NAD^+ for a different analog.

8.3 IoPA and α-KGM Synthesis

In addition to the cofactor studies, the recombinant urocanase was also useful for synthesizing IoPA and α-KGM without complex chemical syntheses. While not utilized here due to timing issues, the immobilized urocanase also has the benefit of being used for multiple syntheses. Storage experiments would need to be done to determine the best way to store immobilized urocanase, but it would reduce the need to frequently purify more urocanase.

The synthesis of IoPA was largely successful in obtaining IoPA separated from urocanate, but there were significant yield issues. Even though 500 micromoles of urocanate were used for the synthesis, only 130 micromoles of IoPA were recovered. Possible areas for improvement include adjusting the conditions to prevent the breakdown of IoPA during the synthesis since it is a very unstable molecule in neutral conditions. The column equilibration and sample preparation conditions should also be optimized to ensure that all of the IoPA is binding to the resin. High absorbances at 230 nm were observed in washes before elution, so there is a likelihood that a lot of IoPA is lost due to improper conditions for strong binding to the column.

However, since IoPA itself is not directly responsible for AAT inhibition, there is not much need to fine-tune its synthesis. Instead, efforts should be directed at increasing yields of α-KGM recovery, seeing as it is the inhibitory molecule. Assuming that all 0.72 millimoles of

urocanate could be converted to α-KGM, the synthesis performed here had a recovery of 0.005 millimoles of α-KGM, or 0.7%. Lyophilization and re-suspension in a small volume of liquid allowed for a high enough concentration to perform kinetic studies with AAT, but given the high stability of α-KGM, it would be beneficial to synthesize a large amount in one sitting for periodic use in following experiments.

In the α-KGM synthesis, column chromatography was used mainly to remove DCPIP, which strongly bound to the resin. To simplify the procedure, the α-KGM was eluted off the column in one large fraction and lyophilized to reduce the volume. Using a gradient elution and collecting fractions would allow for a higher concentration of α-KGM prior to lyophilizing and would potentially remove any impurities. However, the largest barrier to doing this is finding an efficient way to monitor the fractions coming off the column for α-KGM content.

While the IoPA synthesis could be easily followed via absorbance at 230 nm (where IoPA absorbs) and 277 nm (where urocanate absorbs), elution of α-KGM in acetic acid prevented the use of spectroscopic measurements at 223 nm because of extremely high background noise. Adjusting the ketone assay using 2,4-dinitrophenylhydrazine detailed by Krasnikov et al. for a higher-throughput application would allow for determining which fractions contain α-KGM even in the presence of acetic acid. The separation of α-KGM would be more closely followed by this type of quantitative analysis so that only fractions with large amounts of relatively pure α-KGM are pooled.

8.4 Effect of IoPA and α-KGM on AAT

AAT activity was examined closely here because of previous minimal media growth studies and amino acid replacement experiments that indicated IoPA buildup caused AAT inhibition. In *Salmonella,* Bochner & Savageau (1979) showed that internal buildup of IoPA resulted in growth inhibition that could be relieved by the addition of glutamate, but not aspartate. A similar pattern of growth-relief was also observed in *E. coli* mutants lacking AAT (Gelfand & Steinberg, 1977). The IoPA-mediated glutamate starvation could be explained in part by the inhibition of AAT; if nitrogen is assimilated into aspartate, transfer of the nitrogen onto α-ketoglutarate to make glutamate would be prevented (Bochner & Savageau, 1979). However, until this study, the actual inhibition of AAT by an IoPA-breakdown product had not been shown.

While IoPA buildup in the *S. typhimurium* cells caused a reduction in growth accredited to loss of AAT activity, IoPA itself is likely not exerting this effect. Addition of IoPA to *E. coli* AAT assays performed here did not reveal a drop in the activity. Use of the suspected inhibitory breakdown product, α-KGM, displayed high levels of AAT inhibition. This corroborates previous growth studies that only observed toxic IoPA effects in the presence of oxygen, which drives IoPA breakdown into compounds like α-KGM (Kabeer, 2000). Kinetic studies allowed for the confirmation that α-KGM inhibition was through a competitive mechanism, which is logical given the similarity in structure to α-ketoglutarate, an AAT substrate.

The results from assaying AAT from crude extract in the presence of α-KGM are promising, but the use of crude extracts complicates the results. We need to exclude the remote possibility that an unknown compound present in the crude extracts of the AAT enzyme preparations might be inhibiting AAT in addition to what is seen when α-KGM is added to AAT

assays. Purifying AAT would allow for assaying the enzyme only in the presence of the predicted inhibitor. Future work should aim to find a source of pure AAT through cloning that can be used for the assays performed here.

With the confirmation of α-KGM as a competitive inhibitor of AAT, the question of how AAT inhibition causes the previously observed decrease in growth opens up. Given the role AAT plays in energy metabolism, it is possible that its inhibition is due to decreased energy output. In *E. coli* in particular, loss of AAT has been linked to issues with cell cycle regulation caused by decreased levels of initiator protein for chromosome replication (Liu et al., 2014). Looking at the levels of this protein upon internal IoPA build up could provide insight on to the ways in which α-KGM -mediated inhibition of AAT lead to issues with cell growth.

The growth-inhibitory effects of IoPA build up might not be limited to *S. typhimurium* and *E. coli* cells, and could have relevance up to the human level. Given the lack of observed humans with IPase deficiencies and the new observance presented here of AAT inhibition by IoPA breakdown products, it is entirely possible that the reason no such deficiencies have been found is due to the absolute necessity to break down IoPA through productive pathways so that it does not decay into α-KGM. This idea could be further explored by assaying human AAT in the presence of α-KGM, or even testing the viability of IPase knockout or knockdown in a human cell line.

BIBLIOGRAPHY

Bender, R. A. (2012). Regulation of the Histidine Utilization (Hut) System in Bacteria. *Microbiology and Molecular Biology Reviews*, *76*, 565-584.

Biellmann, J. F., Hirth, C. G., Jung, M. J., Rosenheimer, N., & Wrixon, A. D. (1974). Studies with Analogues of Nicotinamide Adenine Dinucleotide. *European Journal of Biochemistry*, *41*, 517-524.

Bochner, B. R., & Savageau, M. (1979). Inhibition of Growth by Imidazol(on)e Propionic Acid: Evidence in vivo for Coordination of Histidine Catabolism with the Catabolism of Other Amino Acids. *Molecular Genetics and Genomics*, *168*, 87-95.

Bradford, M. (1976). A Rapid and Selective Method for the Quantitation of Microgram Quantities of Protein Utilizing the Principle of Protein-Dye Binding. *Analytical Biochemistry*, *72*, 248-254.

Brown, D. D., & Kies, M. W. (1959a). The enzymatic formation of L-hydantoin-5-propionic acid. *Journal of Biological Chemistry*, *234*, 3182-3187.

Brown, D. D., & Kies, M. W. (1959b). The Mammalian Metabolism of L-Histdine II. The Enzymatic Formation, Stabilization, Purification, and Properties of 4(5)-Imidazolone-5(4)-Propionic Acid, the Product of Urocanase Activity. *The Journal of Biological Chemistry*, *234*, 3188-3191.

Consevage, M. W., & Phillips, A. T. (1990). Sequence and analysis of the hutH gene encoding histidine ammonia-lyase in Pseudomonas putida. *Journal of Bacteriology*, *172*, 2224-2229.

Eby, D., & Kirtley, M. E. (1971). Interaction of Nicotinamide-Adenine-Dinucleotide and its Analogs with Glyceraldehyde 3-Phosphate Dehydrogenase. *Biochemistry*, *10*, 2677-2682.

Egan, R., Matherly, L. H., & Phillips, A. T. (1981). Mechanism of Urocanase as Studied by Deuterium Isotope Effect and Labeling Patterns. *Biochemistry*, *20*, 123-137.

Egan, R. M., & Phillips, A. T. (1977). Presence of a Tightly Bound NAD in Urocanase of Pseudomonas putida. *Journal of Biological Chemistry*, *252*, 5701-5707.

Espinos, C., Pineda, M., Martinez-Rubio, D., Lupo, V., Ormazabal, A., Vilaseca, M. A., Spaapen, S. J., Palau, F., & Artuch, R. (2009). Mutations in the urocanase gene UROC1 are associated with urocanic aciduria. *Journal of Medical Genetics*, *46*, 407-411.

Gelfand, D. H., & Steinberg, R. A. (1977). Escherichia coli mutants deficient in the aspartate and aromatic amino acid aminotransferases. *Journal of bacteriology*, *130*, 429–440.

Hernandez, D., & Phillips, A. T. (1994). Ser-143 Is an Essential Active Site Residue in Histidine Ammonia Lyase of Pseudomonas putida. *Biochemical and Biophysical Research Communications*, *201*, 1433-1438.

Hilton, J., Christensen, K., Watkins, D., Raby, B., Renaud, Y., de la Luna, S., Estivill, X., Mackenzie, R., Hudson, T., & Rosenblatt, D. (2003). The molecular basis of glutamate formiminotransferase deficiency. *Human Mutation*, *22*, 67-73.

Kabeer, S. (2000). *Growth inhibition by imidazolone propionic acid (IPA): Evidence for an oxygen dependent mechanism* [Honors Thesis]. Pennsylvania State University.

Kalafatic, Z., Lipovac, K., Jezerinac, Z., Juretic, D., Dumic, M., Zurga, B., & Res, L. (1980). A Liver Urocanase Deficiency. *Metabolism*, *29*, 1013-1019.

Kaupinnen, R., Sirah, T., & Nicholls, D. (1987). Aminooxyacetic acid inhibits the malate-aspartate shuttle in isolated nerve terminals and prevents the mitochondria from utilizing glycolytic substrates. *Molecular Cell Research*, *930*, 173-178.

Kessler, D., Retey, J., & Schulz, G. E. (2004). Structure and Action of Urocanase. *Journal of*

Molecular Biology, 342, 183-194.

Kirsch, J., Eichele, G., Ford, G., Vincent, M., Jansonius, J., Gehring, H., & Christen, P. (1984). Mechanism of Action of Aspartate Aminotransferase Proposed on the Basis of its Spatial Structure. *Journal of Molecular Biology, 174*, 497-525.

Klepp, J., & Retey, J. (1989). The stoichiometry of the tightly bound NAD in urocanase. *European Journal of Biochemistry, 185*, 615-619.

Kornberg, H. L. (1966). The Role and Control of the Glyoxylate Cycle in Escherichia coli. *The Biochemical Journal, 99*, 1-11.

Krasnikov, B. F., Nostramo, R., Pinto, J. T., & Cooper, A. J. (2009). Assay and purification of omega-amidase/Nit2, a ubiquitously expressed putative tumor suppressor, that catalyzes the deamidation of the alpha-keto acid analogues of glutamine and asparagine. *Analytical biochemistry, 391*, 144–150.

La Du, B. (1967). Histidinemia. *The American Journal of Diseases of Children, 113*, 88-92.

Langer, B., Langer, M., & Retey, J. (2001). Methylidene-imidazolone (MIO) from histidine and phenylalanine ammonia-lyase. *Advances in Protein Chemistry, 58*, 175-214.

Lam, W. K., Cleary, M. A., Wraith, J. E., & Walter, J. H. (1996). Histidinaemia: a benign metabolic disorder. *Archives of Disease in Childhood, 74*, 343-346.

Liu, F., Hao, J., Yan, H., Bach, T., Fan, L., & Morigen. (2014). AspC-Mediated Aspartate Metabolism Coordinates the Escherichia coli Cell Cycle. *PLoS ONE, 9*, 1-11.

Magasanik, B., & Bowser, H. R. (1955). The degradation of histidine by Aerobacter aerogenes. *Journal of Biological Chemistry, 213*, 571-580.

Mao, Y., Vyas, N., Vyas, M., Chen, D.-H., Ludtke, S., Chiu, W., & Quiocho, F. (2004).

Structure of the bifunctional and Golgi-associated formiminotransferase cyclodeaminase octamer. *The EMBO Journal*, *23*, 2963-2971.

Margulies, C., & Kaguni, J. M. (1996). Ordered and sequential binding of DnaA protein to oriC, the chromosomal origin of Escherichia coli. *The Journal of Biological Chemistry*, *271*, 17035-17040.

Matherly, L., & Phillips, A. T. (1980). Substrate-Mediated Inactivation of Urocanase from Pseudomonas putida, Evidence for an Essential Sulfhydryl Group. *Biochemistry*, *19*, 5814-5818.

Miesack, B., & Coruzzi, G. (2002). Molecular and Physiological Analysis of Arabidopsis Mutants Defective in Cytosolic or Chloroplastic Aspartate Aminotransferase. *Plant Physiology*, *129*, 650-660.

Rao, R. D., & Greenberg, D. M. (1961). Purification and properties of imidazolone propionic acid hydrolase. *Journal of Biological Chemistry*, *236*, 1758-1763.

Safer, B. (1975). The metabolic significance of the malate-aspartate cycle in the heart. *Circulation Research*, *37*, 527-533.

Song, Y., Ahn, J., Suh, Y., Davis, M., & Lee, K. (2013). Identification of Novel Tissue-Specific Genes by Analysis of Microarray Databases: A Human and Mouse Model. *PLoS ONE*, *8*, 1-17.

Tabor, H., & Mehler, A.H. (1955). [29] Histidase and urocanase. *Methods in Enzymology*, *2*, 228-233.

Tabor, H., & Mehler, A. (1954). Isolation of N-Formyl-L-Glutamic Acid as an Intermediate in the Enzymatic Degradation of L-Histidine. *Journal of Biological Chemistry*, *210*, 559-568.

Tabor, H., Mehler, A. H., Hayaishi, O., & White, J. (1952). Urocanic acid as an intermediate in

the enzymatic conversion of histidine to glutamic and formic acids. *Journal of Biological Chemistry, 196,* 121-128.

Zampieri, M., Horl, M., Hotz, F., Muller, N., & Sauer, U. (2019). Regulatory mechanisms underlying coordination of amino acid and glucose catabolism in Escherichia coli. *Nature Communications, 10,* 1-13.

ACADEMIC VITA

Isabella Ruud
ivr5094@psu.edu // bellaruud25@gmail.com

Education

Pennsylvania State University — Expected Graduation: May 2022
BSc in Biochemistry and Molecular Biology, with honors

Skills

DNA: purification, PCR, restriction enzyme digest, gel electrophoresis, DNA cloning
Protein: purification, chromatography, assay development, specific activity determination
Cell (Bacterial): growth condition optimization, transformation, protein expression
Cell (Eukaryotic): maintenance of DF-1 lines, transfection, antibiotic selection

Research Experience

Undergraduate Researcher — Spring 2019-present
Pennsylvania State University, Biochemistry and Molecular Biology Department

- Led independent project investigating a potentially toxic intermediate in the histidine breakdown pathway using *E. coli* as the model organism
- Developed unique assay to study cofactor specificity in histidine metabolism enzyme urocanase and verified its success using appropriate controls
- Designed and constructed vectors for overexpression of recombinant proteins
- Successfully purified and assayed enzymes in addition to optimizing purification conditions to increase yield and specific activity

Research Assistant — Summer 2021-present
Pennsylvania State University, Animal Science Department

- Constructed CRISPR vectors using restriction-ligation cloning and Gibson Assembly
- Verified transfection of plasmid and success of gene knock out or NHEJ knock in
- Maintained established chicken fibroblast lines through cell culture and passaging
-

Presentations:

WISER/MURE/FERP Undergraduate Research Symposium, Pennsylvania State University, Fall 2019, *Optimizing urocanase production via growth condition of host cells* (poster)

Grants and Awards:

Homer F. Braddock College of Science Memorial Scholarship	Fall 2018- Spring 2022
University Park 4 Year Provost Award	Fall 2018- Spring 2022
Schreyer Honors Academic Excellence Scholarship	Fall 2018- Spring 2022
Evan Pugh Scholar Senior Award	Spring 2021
Office of Science Engagement Grant	Spring 2020
WISER NASA Pennsylvania Space Grant	Spring 2019-Fall 2019